Theoretical and Applied Climatology (2026) 157:311
https://doi.org/10.1007/s00704-026-06253-4

RESEARCH

Urban vegetation loss: assessing built-up expansion and its implications on vegetation cover's health and land surface temperature in the Accra Metropolitan Area, Ghana

Michael Batame[1] · Emmanuel Yeboah[2] · Elisha Njomaba[3] · Isaac Sarfo[4,13] · Selasi Klutsey[5] · Oznur Isinkaralar[6] · Muhammad Waseem[7,14] · Ali Hasan Jaffry[2] · Kaan Isinkaralar[8] · Henry Adjanor Tetteh[9] · Paul Kyeku[10] · Ishmeal Quist[11] · Vincent Awuku[12] · Kaleem Ullah[2] · Augustine O. K. N. Mensah[11]

Received: 7 January 2026 / Accepted: 10 April 2026 / Published online: 18 April 2026

Abstract

Rapid and unplanned urban expansion across sub-Saharan Africa has intensified landscape degradation and surface warming; however, long-term integrated assessments linking land use/land cover (LULC) change, vegetation dynamics, and land surface temperature (LST) remain limited. Addressing this gap, this study analyses land-use/land-cover (LULC) dynamics and their thermal implications in the Accra Metropolitan Area (AMA) from 2000 to 2020, with projections to 2050. Using Landsat imagery within an integrated analytical framework, we combined a random forest classifier for historical LULC mapping, the MOLUSCE CA–ANN model for future scenario simulation, and Geo-detector and K-means clustering to quantify drivers and spatial patterns of thermal variation. Results indicate substantial landscape restructuring: vegetation cover declined from 35.7% in 2000 to 22.7% in 2020 and is projected to decrease to approximately 10.2% by 2050. Concurrently, built-up areas expanded from 62.5% to 75.6%, with projections suggesting continued growth under a business-as-usual scenario. These transitions have substantially increased land surface temperature (LST), as evidenced by a strong negative correlation between NDVI and LST ($r = -0.9$) and a positive correlation between NDBI and LST ($r=0.8$). Spatial analysis identified built-up expansion as the dominant driver of surface warming, with intensifying urban heat island effects concentrated in central and southern AMA. By integrating long-term forecasting with a mechanistic assessment of land-cover change and surface energy dynamics, this study provides actionable evidence for targeted mitigation. Without urgent policy intervention, AMA faces escalating ecological and climatic risks. The findings offer a robust scientific basis for green infrastructure planning and sustainable urban management, aligned with SDGs 11, 13, and 15 in Accra and other rapidly urbanized contexts.

1 Introduction

Rapid urbanization is one of the most dominant drivers of environmental change worldwide, particularly in cities of the Global South, where population growth, infrastructure expansion, and land conversion occur at unprecedented rates (Li et al. 2022; Myers 2021; Seto et al. 2013). As cities expand, urban growth alters land use/land cover (LULC) patterns through the conversion of natural and semi-natural landscapes into built-up environments (Assede et al. 2023; Mir et al. 2025). One of the most immediate consequences of this transformation is the loss and fragmentation of urban vegetation, as green spaces are increasingly replaced by impervious surfaces such as buildings, roads, and other infrastructure.

Vegetation plays a critical role in maintaining ecosystem functionality within urban environments by regulating microclimates, enhancing evapotranspiration, sequestering carbon, and moderating surface and atmospheric temperatures (Hu et al. 2023; Liu et al. 2025; Zhang et al. 2023). However, increasing anthropogenic pressure associated with rapid urban expansion has significantly weakened these regulating functions in many rapidly growing cities,

Extended author information available on the last page of the article

contributing to intensified surface warming and broader ecological stress.

Population growth intensifies demand for housing, transportation networks, commercial infrastructure, and public services, often resulting in the conversion of vegetated and agricultural land into impervious built-up surfaces (Bhattarai and Conway 2020; Chithra et al. 2016). Numerous studies have demonstrated that human-induced land cover change exerts a stronger influence on vegetation dynamics than natural processes, particularly in urban and peri-urban environments (Awotwi et al. 2018; Sarfo et al. 2023a, b, 2024). The environmental consequences of vegetation loss include increased flood risk, soil erosion, biodiversity decline, and intensified land surface temperature (LST), collectively exacerbating urban heat island (UHI) effects (Alademomi et al. 2022; Yeboah et al. 2025).

While some high-income countries have mitigated vegetation loss through effective land-use governance and reforestation initiatives, this trend is not universal. For example, studies in parts of Europe and East Asia have reported stable or increasing urban vegetation cover despite continued population growth, largely due to strong land-use governance, reforestation programs, and institutionalized urban greening policies (Ahmadzai et al. 2022; Anselmetto et al. 2024; Enescu et al. 2025). These outcomes are typically observed in contexts characterized by effective zoning enforcement, long-term environmental planning, and public investment in green infrastructure. However, such institutional and regulatory frameworks differ substantially from those of many rapidly urbanizing cities in sub-Saharan Africa, where informal settlement expansion, weak enforcement mechanisms, and limited urban ecological planning contribute to continued vegetation decline (Awuah and Abdulai 2022; Baye 2025).

In Ghana, urban centres such as Accra, Kumasi, Tamale, and Sekondi-Takoradi have undergone rapid demographic and spatial expansion over recent decades (Abass et al. 2018; Songsore 2020). National assessments indicate substantial loss of vegetation and forest cover, driven primarily by urbanization and land conversion (Acheampong et al. 2022; Oduro et al. 2025). Remote sensing studies have documented these changes across multiple cities. For instance, Frimpong et al. (2024a); Frimpong et al. (2024b) reported significant increases in built-up areas at the expense of vegetation in Kumasi and Accra, while Biney and Boakye (2021) and Sarfo et al. (2022) observed extensive land cover transitions associated with urban sprawl in Sekondi-Takoradi. Similarly, Amekudzi et al. (2024) demonstrated a strong relationship between urban expansion and rising LST in the Greater Accra Region.

Despite these contributions, notable gaps remain in the existing literature. The Accra Metropolitan Area (AMA), Ghana's political and economic hub, represents a critical case due to its rapid urban growth, dense population, and escalating environmental pressures. Many Ghanaian studies are spatially constrained to selected sub-metropolitan areas or river basins, limiting their ability to capture city-wide dynamics (Ackom et al. 2020; Frimpong et al. 2024a). Moreover, most analyses focus on historical land cover change without extending projections beyond 2030, even though longer-term forecasts are essential for climate adaptation and sustainable urban planning (McManamay et al. 2024; Seto et al. 2013). In addition, few studies apply spatial heterogeneity tools such as Geo-detector or clustering algorithms to quantify the relative contribution of different LULC types to spatial variations in LST and vegetation health (Estoque et al. 2017; Wang et al. 2022).

Building on previous studies that have documented historical land-cover dynamics and applied predictive modelling frameworks, this study advances understanding by integrating predictive modelling and spatial heterogeneity analysis to quantify how specific land-use transitions drive vegetation loss and surface warming across the entire Accra Metropolitan Area. By combining multi-temporal Landsat-based LULC analysis (2000, 2010, 2020), long-term projections (2030 and 2050) using the MOLUSCE framework, and advanced spatial analytical techniques (Geo-detector and K-means clustering), this study provides a comprehensive and mechanistic assessment of urban ecological change. The findings offer policy-relevant insights for urban heat mitigation, green infrastructure planning, and climate-resilient urban development, with implications extending to other rapidly urbanizing cities in sub-Saharan Africa.

2 Materials and methods

2.1 Conceptual framework

Environmental change in rapidly urbanizing regions results from the interaction of demographic growth, land-use pressures, and governance responses. This study adopts an integrated conceptual framework to examine how population growth, urban expansion, and policy implementation interact to influence vegetation cover dynamics and land surface temperature (LST) patterns within the Accra Metropolitan Area (AMA) (Attua and Fisher 2011). Figure 1 illustrates these relationships and provides a structured basis for understanding the processes driving vegetation change and surface warming. As shown in Fig. 1, population growth driven by natural increase and migration stimulates urbanization and increases demand for land for residential development and infrastructure. As urban areas expand to accommodate housing and other urban facilities, natural vegetation is

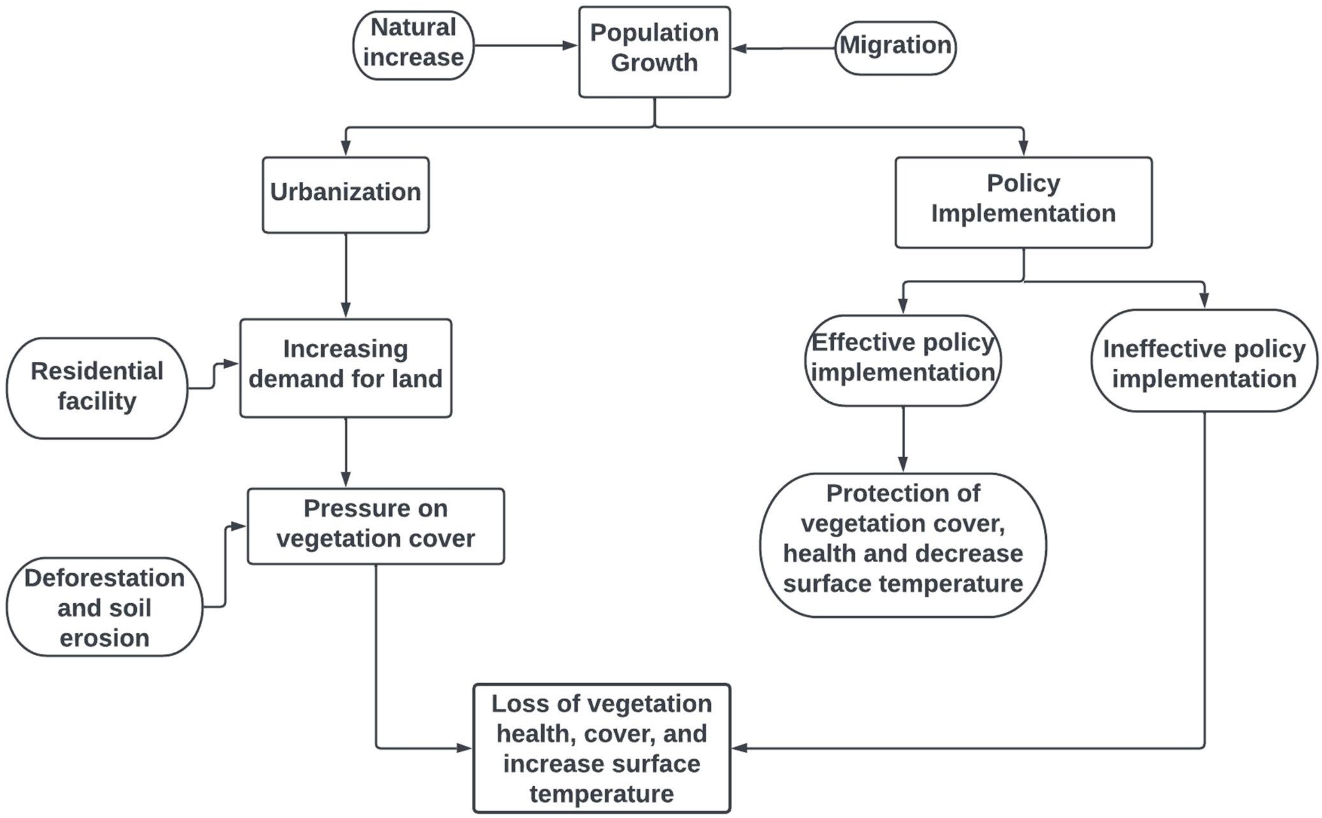

Fig. 1 A conceptual framework illustrating the relationships among population growth, urban expansion, land demand, vegetation loss, and land surface temperature (LST), with policy implementation acting as a moderating factor

increasingly converted into built-up surfaces. This conversion places significant pressure on vegetation cover, resulting in vegetation loss and degradation.

Vegetation plays a critical role in regulating urban microclimates through shading, evapotranspiration, and surface cooling processes. However, vegetation clearing for infrastructure reduces these regulating functions, thereby increasing land surface temperatures. In addition, the removal of vegetation exposes soil surfaces, increasing susceptibility to environmental degradation processes such as soil erosion during intense rainfall events (Yiran et al. 2012). Over time, these processes contribute to declining vegetation health and increased surface temperatures across urban landscapes (Zhang et al. 2023). The framework also recognizes that policy implementation and governance mechanisms can influence these dynamics. Effective urban planning policies and vegetation protection measures can help mitigate vegetation loss and moderate surface temperatures through strategies such as green infrastructure planning and controlled land-use development. Conversely, weak policy enforcement may allow uncontrolled land conversion, further accelerating vegetation degradation and urban heat accumulation. In this way, policy implementation acts as a mediating factor that can either mitigate or exacerbate the environmental impacts of rapid urbanization.

The concept demonstrates that policy implementation can either mitigate or exacerbate the environmental impacts of urban expansion. In several cities, effective policy implementation has helped protect urban vegetation and moderate surface temperatures through green infrastructure planning and urban greening programs. For example, large-scale urban tree planting and green corridor initiatives in cities such as Singapore and Seoul have contributed to improved vegetation cover and measurable reductions in urban heat island intensity (Gill et al. 2007; Tan et al. 2016). Similarly, urban greening policies and ecological restoration programs implemented in Chinese cities have been shown to enhance vegetation cover and reduce surface temperatures (Zhang et al. 2017). Conversely, weak policy enforcement or poorly coordinated urban planning can accelerate vegetation loss and environmental degradation. In many rapidly urbanizing cities in the Global South, limited enforcement of land-use regulations has allowed uncontrolled land conversion and deforestation for infrastructure development, contributing to declining vegetation health and increasing land surface temperatures (Seto et al. 2013; Cobbinah and Aboagye 2017).

2.2 Methodology overview

This study employs an integrated geospatial and machine learning framework to investigate land use/land cover (LULC) dynamics and their impacts on vegetation and land surface temperature (LST) in the Accra Metropolitan Area. As illustrated in Fig. 2, satellite imagery from 2000, 2010, and 2020 was preprocessed using radiometric correction, cloud masking, and area-of-interest clipping. Key environmental indicators, Normalized Difference Vegetation Index (NDVI), Normalized Difference Built-up Index (NDBI), and LST, were derived from the processed imagery. A Random Forest classifier was used to generate LULC maps for each period. These maps were subsequently analyzed using Geo-detector and K-means clustering to quantify spatial relationships between land cover and thermal patterns. Future LULC scenarios for 2030 and 2050 were simulated using the MOLUSCE modelling framework. The combined analyses enabled an integrated assessment of urban heat dynamics and vegetation loss associated with rapid urbanization.

2.3 Study area description

The Accra Metropolitan Area (AMA), the capital and most densely populated city of Ghana, was selected for this study as a highly representative case of rapid, unplanned urbanization in sub-Saharan Africa (Fig. 3) (Abass et al. 2018; Yiran et al. 2020). This research utilizes the historical administrative boundary of the AMA, which covered 139.674 km² and encompassed ten sub-metropolitan districts (Ghana Statistical Service 2014), as this broader spatial extent more effectively captures the core urban agglomeration and the dynamic peri-urban zones experiencing the most intense land use transitions (Cobbinah and Aboagye 2017). Bordered by other rapidly urbanizing municipalities (Ga West, Ga South, La Dadekotopon) and the Gulf of Guinea, the region is a constrained and dynamic urban region (Grant

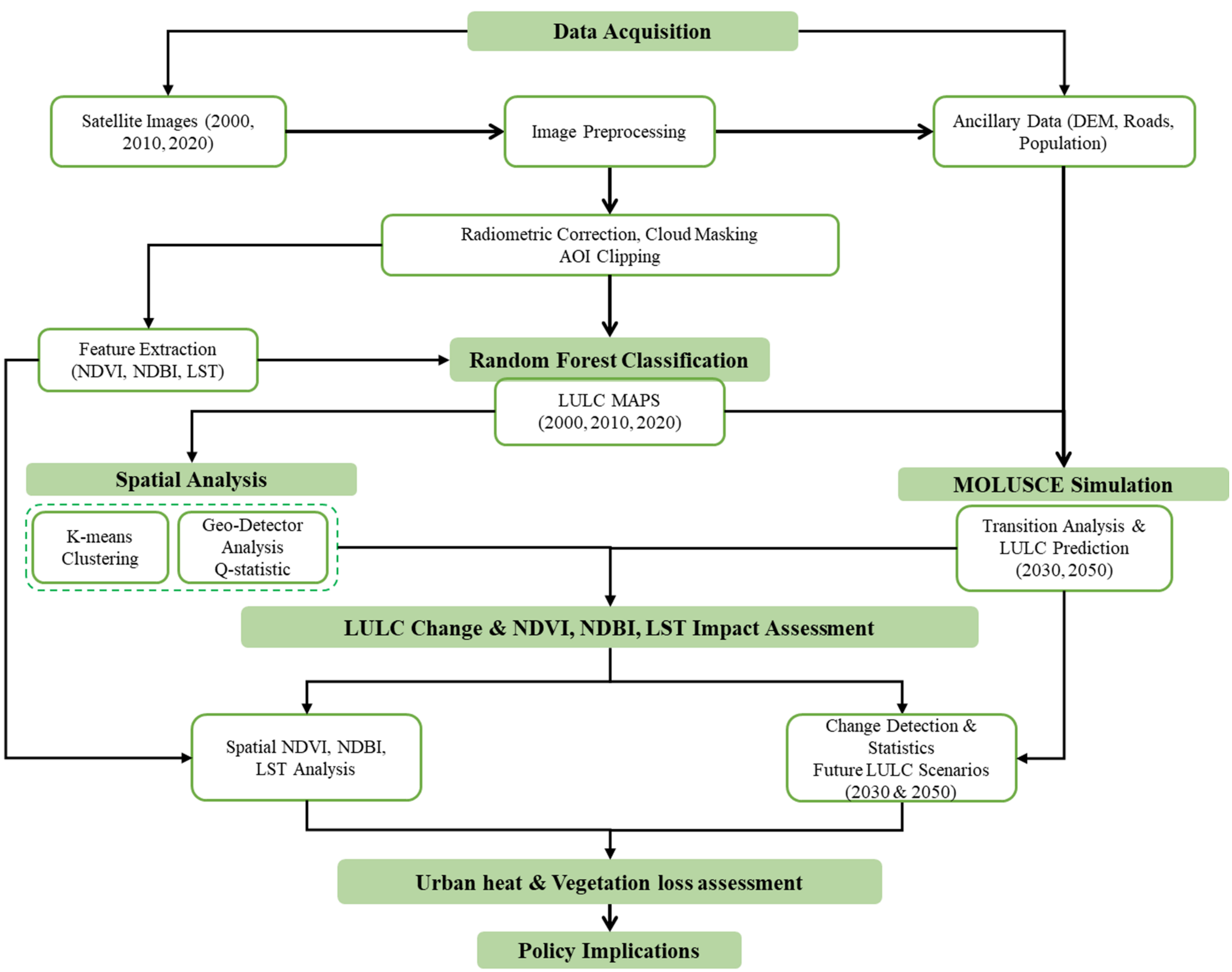

Fig. 2 A methodological workflow of the study

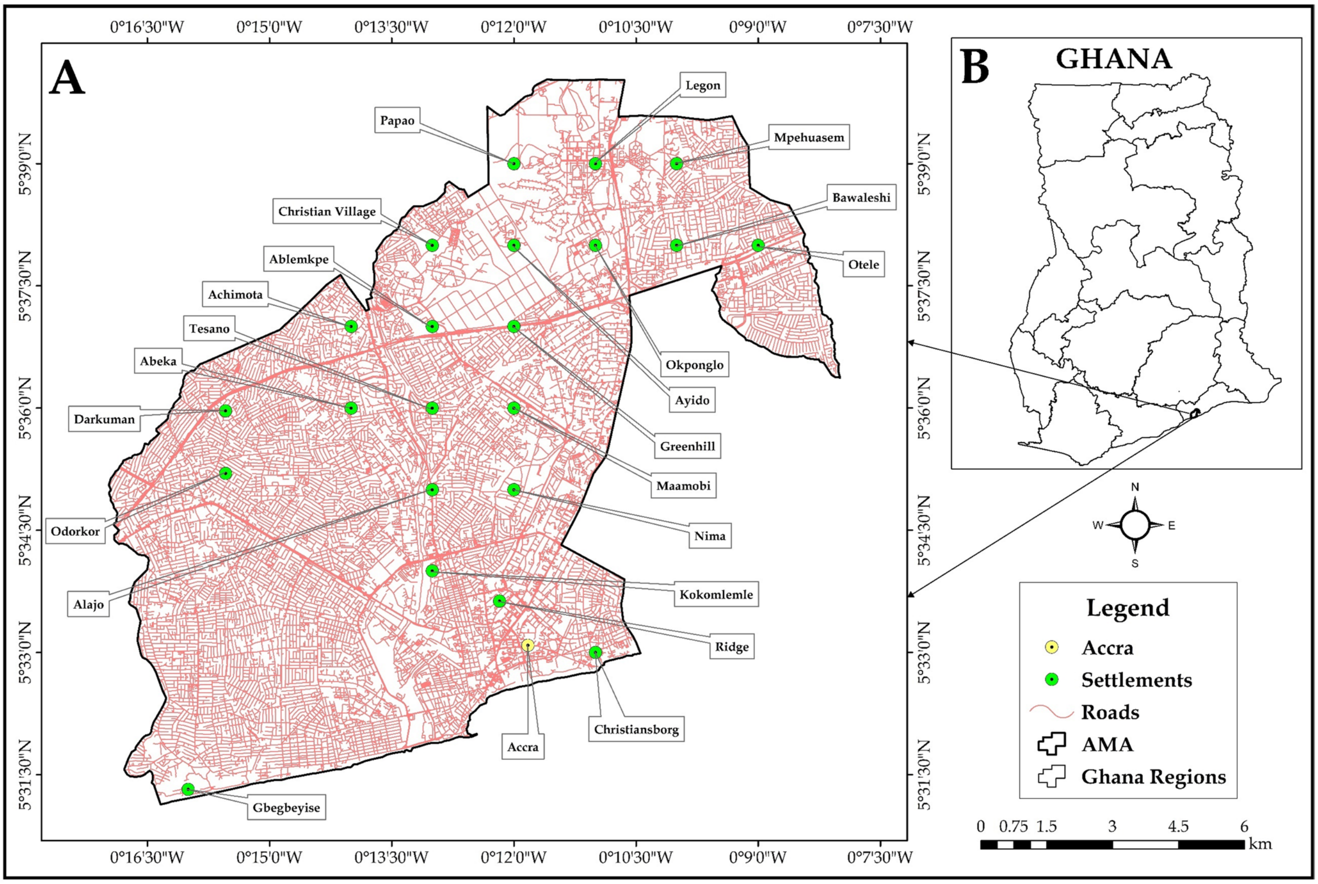

Fig. 3 The location of the study area. (**A**) The Accra Metropolis showing the various towns and Accra as the capital, and (**B**) the Ghana map showing the regional boundaries and AMA's position

and Nijman 2004). Climatically, the area features a tropical savanna climate with an average annual temperature of 26.8 °C and a low annual rainfall of 730 mm (Ansah et al. 2020), supporting diverse vegetation forms including mangroves, grasslands, shrublands, and forests (Acheampong et al. 2018).

As Ghana's primary economic and administrative hub, the AMA exemplifies the powerful pressures driving urban change across the region (Grant and Yankson 2003). The metropolis recorded a population of over 1.66 million in the 2010 Population and Housing Census, with immigrants constituting approximately 47% of residents (Ghana Statistical Service 2014). Although more recent census exercises confirm continued population growth in the metropolis, the 2010 census provides the most recent detailed breakdown of migrant composition. This substantial demographic pressure has contributed to intensified demand for housing and infrastructure (Cobbinah et al. 2015). This has directly catalyzed the massive destruction of vital vegetation cover, making the AMA a critical and generalizable case study for investigating the spatiotemporal dynamics of urbanization, its precise impact on vegetation health, and the resulting increase in land surface temperature (Owusu et al. 2023). The findings from this focused study are therefore directly applicable to similar urban centers throughout sub-Saharan Africa.

2.4 Satellite dataset and processing

Landsat images for the Accra Metropolitan Area were downloaded from the United States Geological Survey (USGS) Earth Explorer portal (https://earthexplorer.usgs.gov/). Level-2 Surface Reflectance products from the Landsat Collection 2 dataset were used, which provide atmospherically corrected and analysis-ready imagery suitable for land cover and surface temperature analysis. The dataset included Landsat 5 Thematic Mapper (TM) imagery for 2000, Landsat 7 Enhanced Thematic Mapper Plus (ETM+) imagery for 2010, and Landsat 8 Operational Land Imager/Thermal Infrared Sensor (OLI/TIRS) imagery for 2020, all from path 193, row 055 of the Worldwide Reference System (WRS-2) and at a 30-meter spatial resolution (Yeboah et al. 2025). To ensure comparability, all images were selected from the dry season (December–February) to minimize atmospheric interference and variations in vegetation phenology. The images were also chosen for their minimal cloud cover and absence of errors, such as scan line corrector (SLC)-off gaps on Landsat 7. The images underwent preprocessing, including radiometric calibration and layer stacking. For visualization and feature interpretation, standard false-color composite band combinations were used, including bands 7 (Mid-Infrared), 4 (Near-Infrared), and 2 (Green) for Landsat 7 ETM+, bands 6 (Shortwave-Infrared 1), 5 (Near-Infrared), and 3 (Green) for Landsat 8 OLI/TIRS, and bands 5 (Mid-Infrared), 4 (Near-Infrared), and 2 (Green) for Landsat 5 TM. These band combinations enhance the discrimination of vegetation, built-up areas, and bare land and are widely used in urban land-cover studies. However, for the Random Forest classification, the full set of available multispectral bands for each sensor, in addition to derived indices (NDVI and NDBI), was used as predictor variables to improve class separability. A total of 100 ground truth points were collected for each period. 70% (70%) of these points were used to train the random forest classification algorithm, while the remaining 30% (30%) were reserved for accuracy assessment. The ground truth samples were selected using a stratified random sampling approach to ensure representation across all four land-use land-cover classes (built-up, vegetation, bare land, and water bodies). Sample points were spatially distributed throughout the study area to capture landscape heterogeneity, and class labels were verified using high-resolution Google Earth imagery and ancillary local knowledge. This stratified design was implemented to minimize class imbalance and ensure that each land cover type was adequately represented in both the training and validation subsets. For the Random Forest classification, the training dataset consisted of the spectral reflectance values extracted from the Landsat imagery at the locations of the reference points. These predictor variables included the Landsat spectral bands used in the analysis as well as derived spectral indices such as the Normalized Difference Vegetation Index (NDVI) and the Normalized Difference Built-up Index (NDBI). The inclusion of both spectral bands and indices improves the discrimination of land cover classes by capturing differences in vegetation density, built-up surfaces, and soil exposure. For each ground truth point, the corresponding pixel values from these bands and indices were used as input features for the Random Forest algorithm, while the associated land cover label served as the target class during model training. The accuracy of the Random Forest classification was assessed using overall accuracy and producer's accuracy. Although NDVI and NDBI were calculated using specific spectral bands, the Random Forest classification utilized the full set of available multispectral bands as predictor variables to improve discrimination between vegetation, built-up areas, bare land, and water bodies. The details of the satellite datasets used are summarized in Table 1.

2.4.1 Processes of LULC prediction

The random forest machine learning algorithm was employed for the land use/cover classification (Breiman 2001). The land use/cover classes included vegetation (all green areas, such as parks, grassland, and forest), bare lands (open land showing soil), built-up (buildings, pavement, roads), and water bodies (Sarfo et al. 2024; Kowe et al. 2021). Within the Accra Metropolitan Area, agricultural land is limited and primarily consists of small peri-urban cultivation plots, which were grouped within the broader vegetation class due to their relatively small spatial extent and similar spectral characteristics in the Landsat imagery. This study used post-classification change detection to detect spatial changes between 2000 and 2020 in the Accra Metropolitan Area. Change detection quantifies, offers changes, and shows the distribution of changing information among classes over time (Sarfo et al. 2023a, b). The accuracy of the classification was assessed by using overall, producer, and user accuracy. The confusion matrix was generated by comparing classified raster outputs with the independent validation dataset. While 30% of the ground truth points were reserved for validation, accuracy assessment was conducted using a confusion matrix comparing classified outputs with reference data. Thus, accuracy metrics reflect pixel-level agreement between classified outputs and reference labels. This clarification ensures distinction between the reference sample size and pixel-based support counts used in accuracy reporting. With this, we initialized

Table 1 Satellite imagery data sources, spatial resolution, and spectral indices used for LULC classification and analysis in the Accra Metropolitan Area

Year	Satellite / Sensor	Bands Used (Classification)	Bands Used (Indices)	Spatial Resolution	Spectral Index	Formula
2000	Landsat 5 TM	Bands 1–5, 7	B4 (NIR), B3 (Red), B5 (SWIR)	30 m	NDVI	(B4−B3) / (B4+B3)
					NDBI	(B5−B4) / (B5+B4)
2010	Landsat 7 ETM+	Bands 1–5, 7	B4 (NIR), B3 (Red), B5 (SWIR)	30 m	NDVI	(B4−B3) / (B4+B3)
					NDBI	(B5−B4) / (B5+B4)
2020	Landsat 8 OLI/TIRS	Bands 1–7, 10–11	B5 (NIR), B4 (Red), B6 (SWIR)	30 m	NDVI	(B5−B4) / (B5+B4)
					NDBI	(B6−B5) / (B6+B5)

the MOLUSCE model with historical data from 2010 to 2020 to project the LULC for the years 2030 and 2050. This simulated map was then quantitatively compared against a ground-truth, independently classified from the historical dataset, which served as the validation benchmark. To validate the predictive performance of the MOLUSCE model, a hindcasting approach was implemented in which earlier LULC maps were used to simulate the land cover distribution for a known reference year. Specifically, the model was first calibrated using historical LULC maps and then used to generate a simulated map for 2020. The simulated 2020 map was subsequently compared with the independently classified 2020 LULC map to evaluate model performance before generating future projections. The comparison was performed using a confusion matrix to calculate key accuracy metrics for each LULC class and the model overall.

Predictions for 2030 and 2050 were derived using Modules for Land Use Change Evaluation (MOLUSCE) integrated into QGIS version 2.18 (Isinkaralar et al. 2023; Kamaraj and Rangarajan 2022). The 2010 and 2020 land cover maps were used to calibrate the model because MOLUSCE simulations require two temporally sequential maps to estimate transition probabilities, and the most recent period was selected to better capture contemporary urban expansion dynamics within the Accra Metropolitan Area. This software tool employs Cellular Automata and Artificial Neural Network (CA-ANN) methodologies alongside simulations (Kamaraj and Rangarajan 2022; Muhammad et al. 2022), which are used to anticipate changes in AMA classes based on land use/cover maps from 2010 to 2020. The analytical process primarily involves evaluating correlation (EC), quantifying area alterations, transition potential computation (TPC) modelling, and validation conducted across four (4) iterations. Baseline data for the predictions include a Digital Elevation Model (DEM), a road raster georeferenced image of AMA, and land ownership records. Principal predictor variables for future projections included only those with available and reliable datasets, specifically Digital Elevation Model (DEM), road network data, and population data. These variables were selected due to their established influence on urban expansion and land use dynamics. Other factors such as climatic variables, household characteristics, and biodiversity, were considered conceptually as potential drivers of land use change but were not explicitly incorporated into the model due to data limitations and inconsistencies in spatial and temporal coverage. Details of the datasets used, including their sources, spatial resolution, and temporal availability, are provided in Appendix Table 6. Demographic projections and economic forecasts are integrated into the modelling process to enhance accuracy and relevance. To account for projection uncertainty, a sensitivity analysis was conducted within the MOLUSCE framework by varying key predictor weights and neighborhood configurations across multiple simulation runs. The variability among simulation outputs was quantified to estimate an uncertainty range of approximately ± 5–7% relative to the central projection estimate. Importantly, projected land cover proportions were constrained by the total available land area within the Accra Metropolitan Area boundary to ensure that the simulated built-up extent does not exceed 100% of the study area. Thus, projection ranges represent physically bounded and plausible scenario outcomes rather than unconstrained extrapolations.

2.5 NDVI and NDBI indices

The Normalized Vegetation Difference Index (NDVI) is one of the indices used to assess the health of vegetation. NDVI is a measurement of the health of a plant based on how it absorbs and reflects light at particular frequencies, and it is mathematically expressed as the difference between the Near Infrared band and the Red band (Faisal et al. 2020). NDVI values range from −1 to 1, where low NDVI values show little or no vegetation potential, while high NDVI values reveal abundant vegetation (Faisal et al. 2020; Hu et al. 2023). Normalized Difference Built-up Index (NDBI) is used to extract built-up features from remote sensing data, like Landsat imagery, and it is calculated by the difference between the Short-wave Infrared (SWIR) band and the Near Infrared (NIR) band (Sarfo et al. 2024). NDBI values range from −1 to 1, where values closer to 1 express a higher density of built-up areas. Moreover, Sarfo et al. (2023a, b) asserted that the integration of NDVI and NDBI enables thorough examination and illustration of shifts in land cover and patterns of urbanization. See Table 1 for the formulas used to calculate the NDVI and NDBI, where B is the Bands of the satellite imagery.

2.6 Land Surface Temperature (LST) analysis

LST is a crucial indicator for numerous environmental issues because it connects land surface fluxes and the surface atmosphere, according to Sarfo et al. (2023a, b). Satellite remote sensing is the most effective method for measuring LST and producing several LST products at the regional and global levels (Zhang et al. 2023). The following three steps, namely digital number (DN) to radiance, radiance to temperature, and temperature to degrees Celsius, were utilized and processed for the LST in ArcMap 10.8.2

2.6.1 Digital number to radiance

The ETM + DN values range between 0 and 255. A conversion of DN to spectral radiance was performed by Sarfo et al. (2022) and Coll et al. (2010) as retrieved from the United States Geological Survey (USGS) Landsat handbook. This calculation is expressed in Eq. 1 below:

$$L_\lambda = \frac{(LMAX_\lambda - LMIN_\lambda)}{QCALMAX - QCALMIN} * (DN - QCALMIN) + LMIN_\lambda \quad (1)$$

where the LMIN and LMAX are the spectral radiances for each band at DN values ranging from 1 to 255 for Landsat 5 TM and Landsat 7 ETM+, and from 1 to 65,535 for Landsat 8 OLI/TIRS. DN is the pixel DN value, and λ is the wavelength. This was performed using ArcGIS 10.8.2

2.6.2 Radiance to temperature

After that, the Temperature (T) in Kelvin (K) was acquired using the below formula in ArcGIS 10.8.2 λ.

$$\mathbf{BT} = \frac{K_2}{\mathbf{In}[(\frac{\mathbf{K1}}{\mathbf{L\lambda}}) + 1]} \quad (2)$$

where BT is the brightness temperature, K2 and K1 are thermal band calibration constants, and Lλ is the calibrated radiance band (Eq. 1). For Landsat 7 (ETM+), K1 is 666.09, and K2 is 1282.71, whereas for Landsat 5 (TM), K1 is 607.76 and K2 is 1260.56 (Ghulam and Hall 2010). This is like Landsat 8 OLI/TIRS: where BT is the brightness temperature, K2 (1321.08) and K1 (774.89) are the thermal constants, band 10, and Lλ is the calibrated radiance band that is Eq. 1 (Avdan and Jovanovska 2016).

2.6.3 Temperature to degree celsius

Since the temperature is required to be in Degrees Celsius (**°C**), the results for the various temperatures must be converted from Kelvin (**K**) to Degrees Celsius (**C**). The formula is shown below

$$\mathbf{Degree\ Celsius}\ (^\circ\ \mathbf{C}) = \mathbf{Kelvin}\ (\mathbf{K}) - 273.15 \quad (3)$$

Radiometric calibration was performed using sensor-specific gain and bias parameters obtained from USGS metadata to convert digital numbers (DN) to spectral radiance prior to temperature retrieval. This process corrects sensor-related radiometric distortions and ensures inter-temporal consistency among Landsat sensors. While a full atmospheric radiative transfer correction was not implemented, images were selected from cloud-free dry-season conditions to minimize atmospheric variability. Surface emissivity was not spatially adjusted using a variable emissivity model; therefore, derived LST values are interpreted as relative surface temperature patterns suitable for comparative spatiotemporal analysis rather than absolute thermodynamic surface temperatures. The consistent application of the same methodology across all years ensures that observed temperature differences reflect land cover change dynamics rather than processing artifacts.

2.7 Analysis of LST, NDVI, and NDBI relationship

The correlation between LST, NDVI, and NDBI from 2000 to 2020 was examined in ArcMap 10.8.2 and Microsoft Excel. The Fishnet tool created 40 rows and 40 columns with the study area shapefile as the template extent. This configuration produced grid cells of approximately 1 km × 1 km across the Accra Metropolitan Area. The Fishnet grid was used to aggregate pixel-level values of NDVI, NDBI, and LST into larger spatial units to reduce pixel-scale variability and spatial autocorrelation, thereby facilitating statistical analysis such as correlation analysis, Geo-detector modelling, and K-means clustering. Edge cells that extended beyond the study area boundary were clipped using the study area shapefile to ensure that only pixels within the Accra Metropolitan Area were included in the analysis. The extract multi-values to point tool was used to generate values from the input raster datasets, namely the NDVI, NDBI, and LST for the various years. Moreover, the clip tool was utilized to extract the extent of the LST, NDVI, and NDBI values within the study area. These values were exported to Excel to create a scatter plot to show the relationship between LST and NDVI, LST and NDBI, and NDBI and NDVI. In addition to the visual scatter plots, the Pearson correlation coefficient (r) was calculated to quantify the strength and direction of the relationships between these variables. To ensure consistency across indices, NDVI, NDBI, and LST were initially computed at the native 30 m × 30 m resolution of Landsat imagery, which served as the minimum analysis unit for spectral calculations. For neighborhood-level statistical summaries, including correlation and clustering analyses, values were subsequently aggregated into 1 km × 1 km grid cells to reduce pixel-level spatial autocorrelation and variability. While NDVI, NDBI, and LST were initially derived from the original 30 m Landsat imagery, the aggregated 1 km grid values were used for the statistical analyses to capture broader spatial patterns and improve the robustness of the statistical relationships. This dual-scale approach enabled the capture of both fine-scale spectral relationships and broader spatial heterogeneity within the Accra Metropolitan Area.

While NDVI is widely used to assess vegetation health, it is known to suffer from saturation in high-biomass areas. In the Accra Metropolitan Area, which is dominated by fragmented vegetation rather than dense closed-canopy forest, the likelihood of significant NDVI saturation was relatively low. To further minimize this limitation, we interpreted

NDVI trends alongside NDBI and LST patterns, ensuring consistency across indicators. We also note that future work could incorporate alternative indices such as the Enhanced Vegetation Index (EVI), which is less sensitive to saturation. Pearson's correlation coefficient (r) was used to quantify the linear relationship between LST, NDVI, and NDBI. To reduce spatial autocorrelation and pixel-level pseudoreplication effects inherent in 30 m Landsat data, correlation analyses were conducted using aggregated 1 km × 1 km grid cells rather than individual pixels. This aggregation reduces local spatial dependency and provides more robust estimates of large-scale spatial associations. Nevertheless, we acknowledge that some degree of spatial autocorrelation may persist in gridded environmental data; therefore, reported correlation values should be interpreted as measures of spatial association rather than strict statistical independence.

2.8 Geo-detector and clustering analysis

A geo-detector was employed to quantify the spatial variation between LST and changes in LULC variables, providing a robust framework for evaluating the influence of different land cover types on LST distribution. By leveraging Geo-detector's capability to analyze spatial heterogeneity, we were able to isolate and measure the contribution of specific LULC change types, such as built-up areas, vegetation, bare land, and water bodies to variations in LST. This approach allowed for a nuanced understanding of the extent to which each land cover category influences thermal dynamics within the Accra Metropolitan Area.

$$\boldsymbol{q} = \frac{\sum_{\boldsymbol{a}=1}^{\boldsymbol{L}} \boldsymbol{U} \boldsymbol{a}\, \boldsymbol{\sigma}_{\boldsymbol{a}}^{2}}{\boldsymbol{U}\, \boldsymbol{\sigma}^{2}} \tag{4}$$

where L is the number of strata of X and U is the number of units that compose the study area, for the stratum α , it is composed of $U\,\alpha$ units; and σ_{α}^{2} and σ^{2} are the variances of X in the stratum α in the study area. In this study, the dependent variable (Y) represents the spatial distribution of land surface temperature (LST), while the explanatory variable (X) represents land cover characteristics, including built-up areas, vegetation, bare land, and water bodies derived from the LULC dataset.

The q statistic measures the explanatory degree of X to Y. If q = 0 suggests the distribution of Y has no connection with X, and a value of q = 1 means the distribution of Y is completely determined by X. The q-statistic ranges from 0 to 1 and represents the proportion of spatial variance in the dependent variable (LST) that can be explained by a given explanatory factor (e.g., built-up area or vegetation). A higher q-value indicates stronger explanatory power and greater spatial stratified heterogeneity, meaning that the spatial distribution of the explanatory variable aligns closely with the spatial pattern of LST. Conversely, q-values closer to 0 suggest weak explanatory influence. Thus, the q-statistic quantifies how much of the observed spatial variation in LST can be attributed to differences in land use/land cover characteristics.

Additionally, K-means clustering was utilized to detect and classify spatial patterns within the LULC change dataset, offering deeper insights into the spatial and temporal clustering of land cover types. The clustering analysis was performed using grid-level variables derived from the Random Forest–classified LULC maps and associated spectral indices. Specifically, NDVI, NDBI, and LST values aggregated at the 1 km × 1 km grid resolution were used as the input variables for the clustering algorithm. These variables capture vegetation condition, built-up intensity, and surface thermal characteristics, allowing the clustering procedure to identify spatially coherent thermal–ecological zones within the Accra Metropolitan Area. This clustering approach provided a high-resolution categorization of LULC change zones, allowing us to group areas with similar land cover characteristics and assess how these clusters correlated with variations in surface temperature. Through the integration of Geo-detector and K-means clustering, we developed a comprehensive methodological framework that not only measures but also visualizes the spatial relationships and clustering tendencies across different land cover types. K-means clustering was applied to standardized grid-level variables, including LST, NDVI, and NDBI values aggregated at 1 km × 1 km resolution. Before clustering, all variables were normalized to ensure equal weighting in Euclidean distance computation. The optimal number of clusters (k = 4) was determined using the elbow method based on within-cluster sum of squares, where diminishing reductions in variance indicated an appropriate cluster solution. Cluster robustness was further assessed using silhouette coefficients, with values ranging from 0.5 to 0.7, indicating moderate to good separation between clusters, a reasonable outcome given the heterogeneous nature of urban land cover patterns. K-means clustering was implemented as a separate analysis for each year (2000, 2010, and 2020) using standardized grid-level variables (NDVI, NDBI, and LST). The resulting clusters represent composite thermal–ecological zones rather than individual land cover classes, capturing variations in vegetation, built-up intensity, and surface temperature across the study area. To ensure meaningful thermal differentiation, mean LST values were compared across clusters, confirming that clusters characterized by higher vegetation indices corresponded to lower mean surface temperatures relative to built-up dominant clusters.

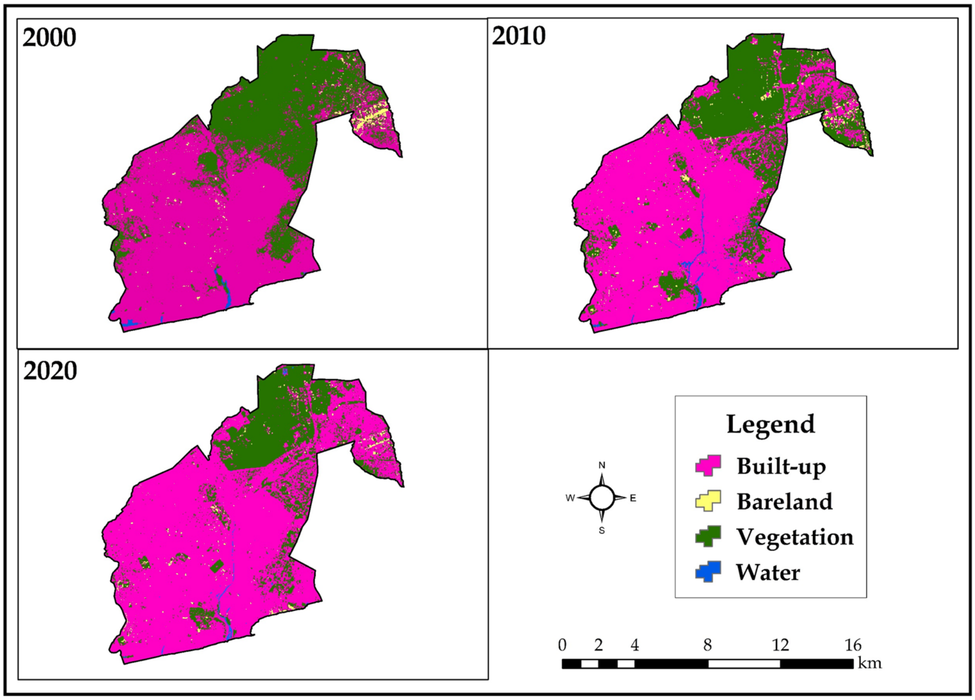

Fig. 4 Classified LULCC maps of the Accra Metropolitan Area in 2000, 2010, and 2020, derived from Landsat imagery using the random forest classifier

Table 2 Historical (2000–2020) and projected (2030–2050) LULC statistics of the Accra Metropolitan Area (km² and %)

LULC Classes	2000	2010	2020	2030	2050
Built-up	87.3 (62.50%)	93.3 (66.81%)	105.59 (75.40%)	117.88 (82.60%)	131.22 (89.70%)
Bare land	1.82 (1.30%)	2.23 (1.60%)	1.68 (1.20%)	0.98 (0.70%)	0.46 (0.31%)
Vegetation	49.86 (35.70%)	42.88 (30.79%)	31.71 (22.60%)	23.33 (16.30%)	14.25 (9.79%)
Waterbodies	0.69 (0.50%)	1.12 (0.80%)	1.12 (0.80%)	0.59 (0.40%)	0.31 (0.20%)

3 Results

3.1 LULC classification results

The AMA landscape underwent a marked spatial change from 2000 to 2020, particularly regarding classes such as built-up and vegetation (Fig. 4; Table 2). Figures 4 and 5 present the spatial distribution of the LULC classes in the study area across the studied years.

Table 2 summarizes the historical (2000–2020) and projected (2030–2050) LULC statistics for the Accra Metropolitan Area. The overall classification accuracy for the 2000, 2010, and 2020 LULC maps was 80%, 85%, and 88% (Table 3). The reported "Support (pixels)" values in Table 3 correspond to the total number of classified pixels per class derived from the raster map rather than the number of validation points. In 2000, vegetation accounted for 35.7% of the study area, compared to 62.5% for built-up surfaces. By 2010, vegetation had declined to 30.7%, while built-up areas increased to 66.8%. This expansion accelerated between 2010 and 2020, when vegetation decreased further to 22.7%, and built-up surfaces reached 75.6%, representing a decadal increase of 12.29 km² in impervious cover. The increase in built-up area was 6.0 km² between 2000 and 2010, and 12.29 km² between 2010 and 2020, indicating an acceleration of urban expansion during the second decade. Bare land and waterbodies exhibited relatively minor changes throughout the study period. Model projections suggest a continued decline in vegetation and an increase in built-up areas by 2030 and 2050 under a business-as-usual scenario, though these projected values should be interpreted within the model's uncertainty range.

The LULC projection indicated that built-up areas are likely to increase to approximately 84% by 2030 and 94% by 2050 under a business-as-usual scenario (Table 2). However, it is important to note that this value represents a theoretical maximum expansion trend generated by the MOLUSCE model, rather than an absolute prediction. In practice, several geographical and regulatory constraints, including water bodies, wetlands, coastal buffer zones, and protected areas, cannot be converted into urban land, which will limit the total proportion of land that can realistically be developed. Furthermore, to account for model uncertainty, we conducted a sensitivity analysis by varying predictor weights and neighborhood configurations within MOLUSCE. Predictor weights were systematically adjusted within a ± 10–15% range relative to their baseline values to evaluate the influence of individual driving factors on

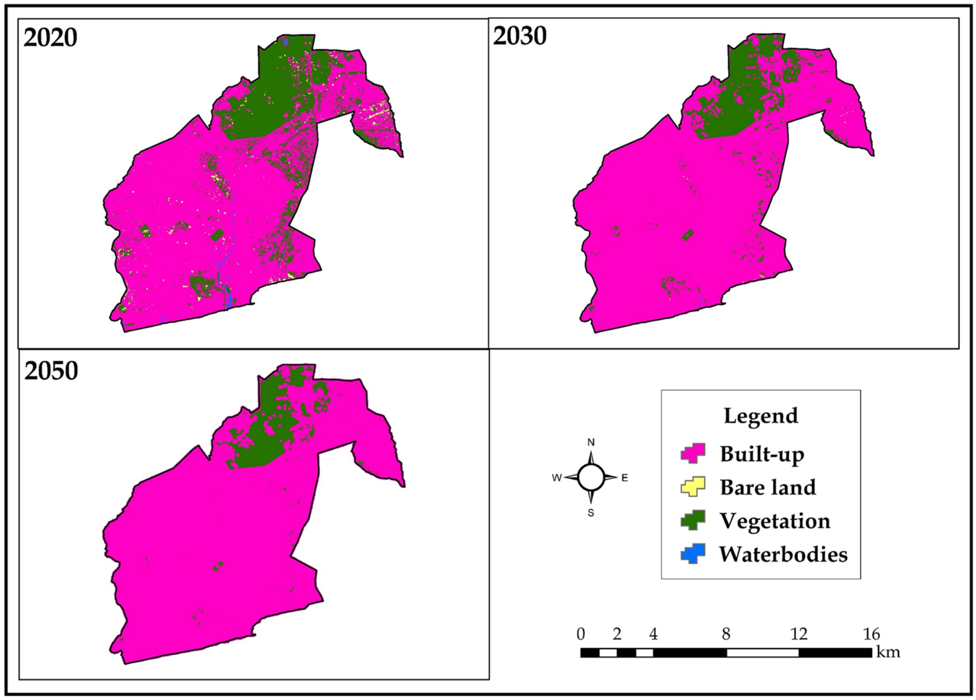

Fig. 5 Predicted LULCC maps for the Accra Metropolitan Area in 2030 and 2050, based on MOLUSCE modelling. The projections indicate continuous expansion of built-up areas and a marked decline in vegetation cover

Table 3 Accuracy assessment of the simulated 2020 LULC map generated by the MOLUSCE model using the independently classified 2020 LULC map as the reference dataset

LULC classes	Precision	Producer's Accuracy	F1-Score	Support (pixels)
Built-up	0.92	0.89	0.91	15,420
Bare land	0.83	0.86	0.84	92,550
Vegetation	0.87	0.88	0.88	205,830
Water	0.81	0.77	0.79	45,200
Overall Accuracy		85.0%		
Kappa Coefficient		0.82		
Macro Avg. F1-Score		0.85		

model outputs. Neighborhood configurations were varied by modifying the neighborhood size parameters used in the cellular automata transition rules, testing multiple configurations to examine how spatial interaction effects influence land cover transitions. In total, multiple simulation runs were performed under these alternative parameter settings, and the variability across the resulting simulations was used to estimate the uncertainty range of the projected land cover outcomes. These alternative runs produced differences of approximately ± 5–7% in the projected extent of built-up area by 2050. Accordingly, the built-up projection should be interpreted within a confidence range of approximately 87–97%, with 94% representing the central estimate and the upper bound constrained by total land availability within the AMA. This range highlights both the robustness and the uncertainty of the model outputs and ensures that the findings are not misinterpreted as exact values but as plausible future scenarios. These clarifications reinforce that while rapid urbanization is expected to continue, the exact magnitude of built-up expansion will depend on policy interventions, land management practices, and the enforcement of environmental regulations.

3.1.1 Validation

The validation results summarized in Table 3 represent the comparison between the MOLUSCE-simulated 2020 LULC map and the independently classified 2020 map derived from the Random Forest model. This comparison evaluates the performance of the MOLUSCE model in reproducing observed land cover patterns. The validation results demonstrate a high degree of model accuracy, with an Overall Accuracy of 85%, indicating a high proportion of correctly classified pixels across the entire map, supported by a Kappa Coefficient of 0.82, which signifies an "almost perfect" agreement between the simulated and actual maps beyond chance. A nuanced view of model performance is provided through class-specific metrics, where the high F1-scores for Water (0.90) and Built-up (0.87) classes indicate exceptional reliability in predicting these stable and rapidly expanding features, respectively, while the slightly lower but still strong scores for Vegetation and Bare land are expected due to their dynamic and transitional nature, a common challenge in LULC modeling. These robust validation results, obtained from the comparison between the simulated 2020 LULC map and the independently classified 2020 map, confirm that the MOLUSCE model is well

Table 4 Land use/land cover transition matrix (%) showing the proportion of land area converted between classes in the Accra Metropolitan Area between 2000 and 2020. Values represent the percentage of the 2020 land cover class that originated from each 2000 land cover class

Initial State (2000)	Water bodies (2020)	Bare land (2020)	Built-up (2020)	Vegetation (2020)
Water bodies	71.25	0.00	0.28	0.61
Bare land	3.86	38.42	15.37	3.24
Built-up	14.92	21.36	78.94	6.85
Vegetation	9.97	40.22	5.41	89.30
Column Total (%)	100	100	100	100

Table 5 Net change of the classes

Class	Net Change (%)
Water bodies	-13.03
Bare land	-2.56
Built-up	+21.02
Vegetation	-36.45

calibrated and effectively captures complex spatial transition dynamics, particularly the critical conversion of vegetation and bare land to built-up areas within the Accra Metropolitan Area, thereby providing confidence in the reliability of the future projections for 2030 and 2050.

3.2 LULC change detection analysis results

The results presented in Table 4 reveal significant land use and land cover transitions in the Accra Metropolitan Area between 2000 and 2020, with vegetation experiencing the most pronounced decline. Vegetation decreased by 36.45% over the study period, reflecting substantial pressure from urban development and land conversion. Although a large proportion of vegetation in 2020 remained unchanged from 2000 (89.30%), a portion was converted into other land cover types, particularly built-up areas (5.41%) and bare land (40.22%), indicating vegetation clearing associated with urban expansion and land preparation activities. In contrast, built-up areas increased markedly by 21.02%, representing the largest net gain among all land cover classes. Most built-up areas in 2020 persisted from previously developed areas (78.94%), while additional expansion occurred through the conversion of bare land (15.37%) and vegetation (5.41%), highlighting the progressive transformation of undeveloped land into urban infrastructure.

Other land cover classes showed relatively smaller but notable changes during the study period. Bare land declined slightly by 2.56%, although the transition matrix indicates that bare land in 2020 originated from multiple sources, including vegetation (40.22%), built-up areas (21.36%), and areas that remained bare land (38.42%), suggesting transitional surfaces associated with vegetation clearing, construction activities, and redevelopment processes. Water bodies also experienced a net decrease of 13.03%, although the majority of water areas remained stable (71.25% persistence). Smaller proportions of water bodies in 2020 originated from built-up areas (14.92%), vegetation (9.97%), and bare land (3.86%), likely reflecting localized hydrological changes or classification mixing along water boundaries.

Overall, the transition patterns highlight a clear trajectory of urban expansion accompanied by substantial vegetation loss, reinforcing the dominant role of built-up growth in shaping land cover dynamics within the Accra Metropolitan Area during the 2000–2020 period (Table 5).

3.3 Spatiotemporal variation of NDVI and NDBI in AMA

The NDVI results showed not only a decline in overall vegetation health but also a clear spatial concentration of low NDVI values in the central and southern portions of AMA, where dense built-up areas dominate (Fig. 6). By contrast, relatively higher NDVI values persisted in the northern peri-urban fringes, particularly around Ga West boundary zones, where agricultural and open green spaces remain. Between 2000 and 2020, areas with NDVI values below 0.1 expanded southwards and eastwards, reflecting progressive loss of vegetated patches in the urban core.

Similarly, the NDBI results revealed a strong spatial differentiation (Fig. 7). High NDBI values (>0.4), indicative of intense built-up concentration, were clustered in central Accra, Osu Klottey, and the coastal sub-metros, while negative or near-zero values were associated with the northern peri-urban zones where vegetative cover was relatively intact. This spatial pattern highlights the north–south gradient of urban sprawl and the corresponding loss of vegetative buffers.

The LST distribution also exhibited distinct spatial differentiation. The highest temperatures (>32 °C) were consistently recorded in the southern and central AMA, particularly in heavily urbanized districts such as Ashiedu Keteke and Ablekuma South (Abass et al. 2018; Yiran et al. 2020). These high-LST zones correspond closely with high-NDBI clusters, confirming the thermal impact of dense built-up areas. In contrast, cooler zones with LST values below 25 °C were observed in the northern fringe communities and along vegetated corridors, particularly near remaining grassland and agricultural plots.

From 2000 to 2020, the spatial expansion of high-LST clusters radiated outward from the urban core, reducing the extent of cooler vegetated zones. This indicates a progressive intensification of the urban heat island effect, with the loss of green spaces directly contributing to localized warming.

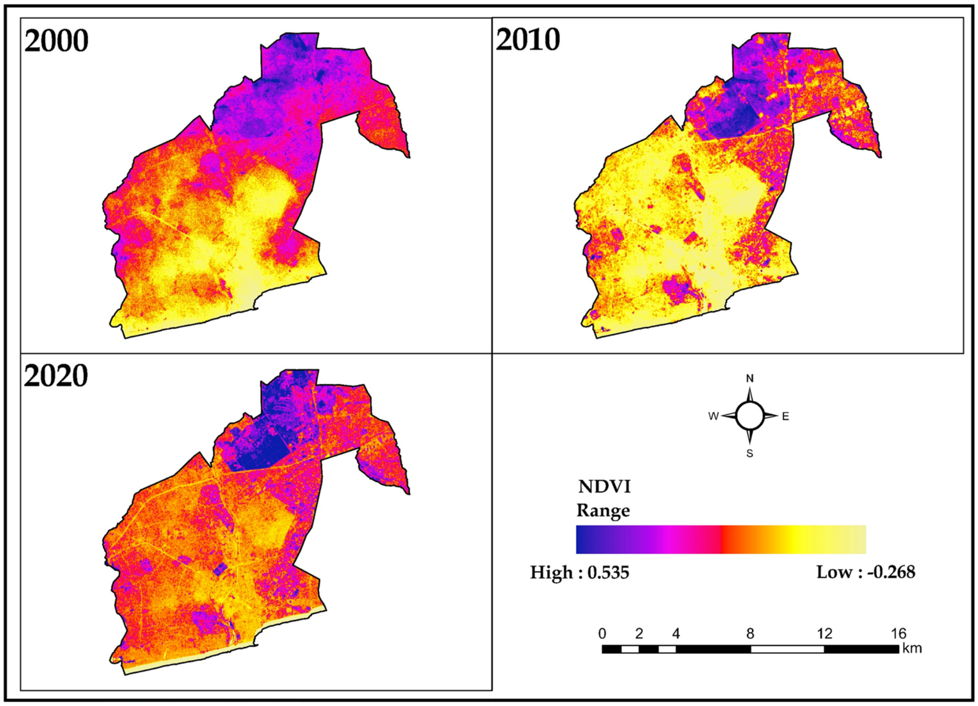

Fig. 6 Spatial distribution of NDVI in the Accra Metropolitan Area for 2000, 2010, and 2020

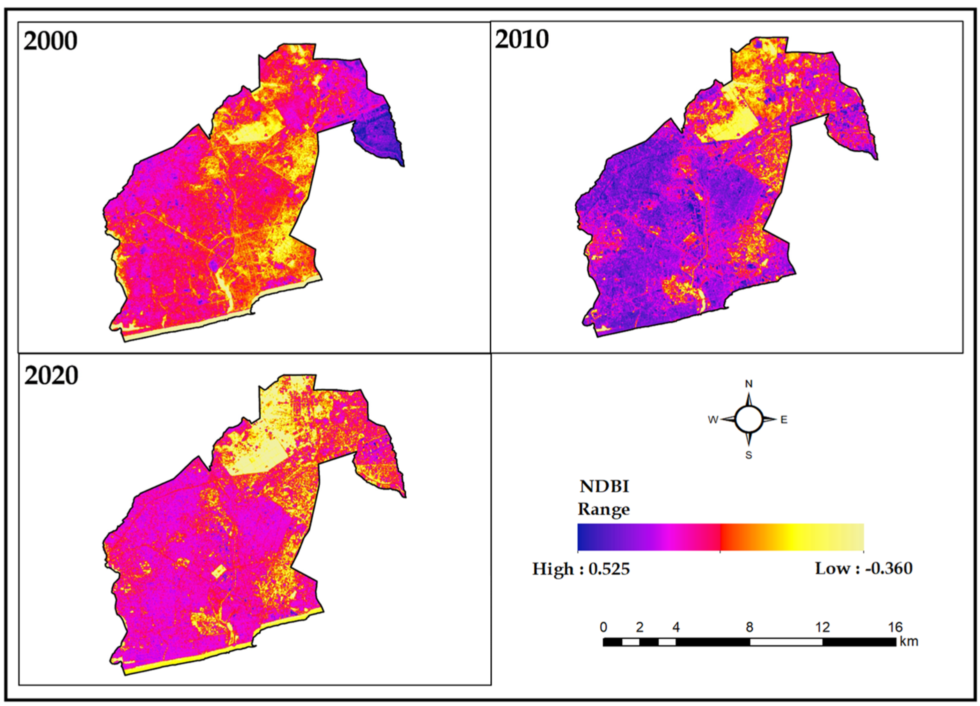

Fig. 7 Spatial distribution of NDBI in the Accra Metropolitan Area for 2000, 2010, and 2020

3.4 Spatiotemporal variation of LSTs in AM

The LST performed for 2000, 2010, and 2020 for AMA (Fig. 8) showed that the temperature in AMA has been increasing steadily. The 2000 LST values for low were 21.4 °C, and high were 32.1 °C. The values for 2010 low and high were 17 °C and 32.9 °C, respectively. The LST 2020 also found that the value for low LST was 20.3 °C and high was 32.5 °C.

3.5 Correlation between LST, NDVI, and NDBI in the study area

The results in Fig. 9 showed that NDVI and LST exhibited a strong negative relationship, indicating that areas

Fig. 8 Spatial distribution of LST in the Accra Metropolitan Area for 2000, 2010, and 2020

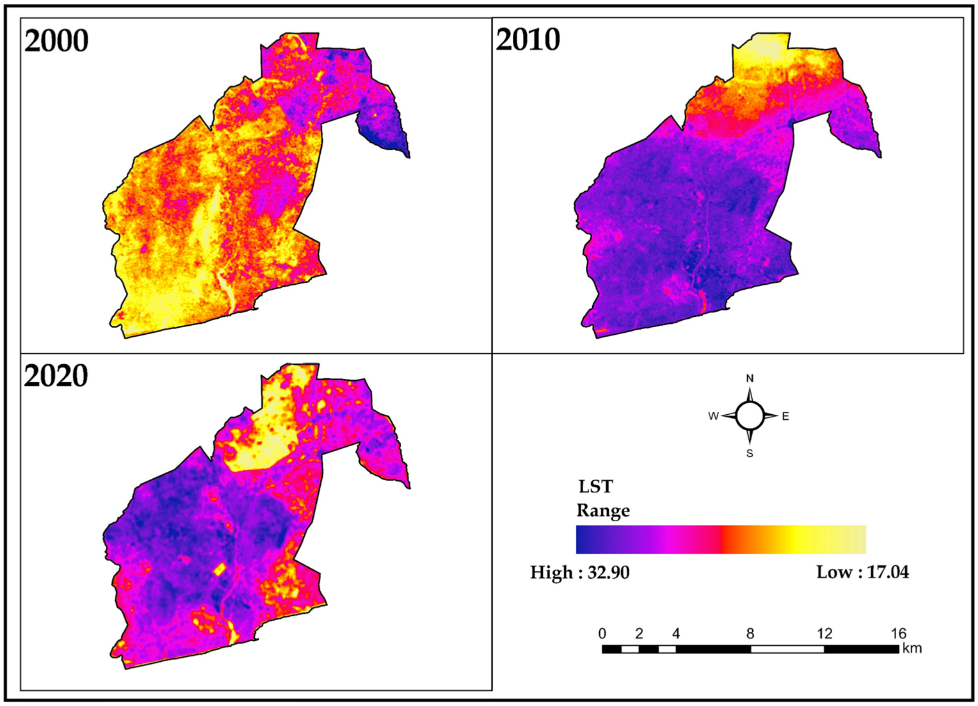

with higher land surface temperatures tend to have lower vegetation density (r = −0.9). In contrast, LST and NDBI displayed a strong positive association (r = 0.8), suggesting that areas characterized by higher built-up intensity are generally associated with higher surface temperatures. Furthermore, NDVI and NDBI exhibited a negative relationship (r = −0.7), indicating that areas with increased built-up surfaces tend to correspond with reduced vegetation cover.

3.6 Geo-detector and clustering analysis

The spatial analysis results of LST in the AMA, as presented in the q-statistics maps (Fig. 10), revealed distinct patterns of land cover influence, shedding light on the dynamics of urban thermal variation. Over the study period from 2000 to 2020, built-up areas (ΔBt) exhibited a consistently increasing impact on LST (Fig. 10a), particularly around the urban core and extending outward as urbanization progressed. The q-statistic values for built-up areas demonstrated the intensifying UHI effect. Vegetation (ΔVg) presented a contrasting effect, where its influence on moderating LST is visible but appears to decline over the years (Fig. 10b). Bare land (ΔBL) consistently exhibited moderate to high q-statistics values across the years, reflecting its steady contribution to increased LST (Fig. 10c). Water bodies (ΔWt), including coastal and riverine areas, display the lowest q-statistics values, signifying a minimal influence on LST compared to other land cover types (Fig. 10d). The circles shown in Fig. 10 represent representative grid cells used to visualize the spatial explanatory power of land-cover variables on LST derived from the Geo-detector analysis. Each circle corresponds to a 1 km × 1 km analysis unit where the q-statistic was computed. The size and color of the circles indicate the magnitude of the q-statistic, reflecting the strength of the spatial association between LST and each land-cover feature. These locations were selected to illustrate spatial variability in explanatory power across the study area rather than to represent individual observation points.

The K-means clustering analysis, applied to standardized grid-level variables including LST, NDVI, and NDBI, revealed distinct spatial clusters representing different combinations of thermal conditions and land-cover characteristics across the Accra Metropolitan Area (Fig. 11). Over the study period (2000–2020), built-up areas (ΔBt) emerged as the primary drivers of elevated LST (Fig. 11a). The clustering results showed a steady outward expansion of high-temperature clusters, particularly in the central and southern zones of Accra. This trend underscores the intensifying UHI effect driven by urban sprawl, in which impervious surfaces like roads and buildings absorb and retain heat. The progression of dark red (cluster 4) and orange (cluster 3) from the city center highlights the growing influence of built-up land on LST (Fig. 11b). Cluster 4 represents areas characterized by the highest LST values, high NDBI, and low NDVI, indicating dense built-up surfaces with limited vegetation cover. Cluster 3 represents moderately urbanized areas with elevated LST and intermediate NDBI values, reflecting mixed land-use zones where built-up areas coexist with fragmented vegetation. In contrast, clusters 1 and 2 are associated with lower LST values and higher

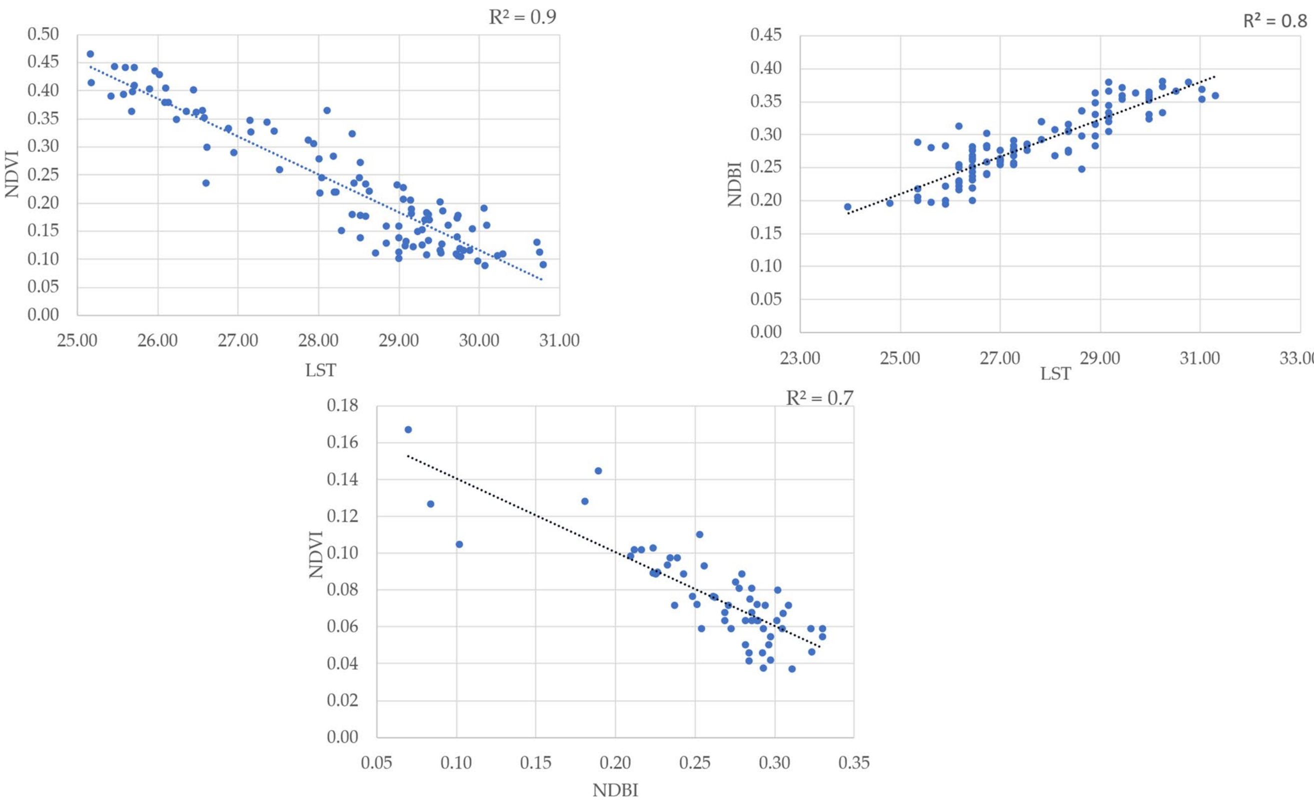

Fig. 9 Graphs showing the correlation between NDVI, NDBI, and LST for the Accra Metropolitan Area across the study years (2000, 2010, 2020)

NDVI, representing areas with greater vegetation cover and reduced built-up intensity. These spatial patterns highlight the increasing influence of urban expansion on surface thermal dynamics, with implications for urban resilience and public health as temperatures rise. Vegetation (ΔVg) clusters presented a contrasting pattern, showcasing the natural cooling potential of green spaces. However, the analysis revealed a decline in vegetation's spatial extent over time, particularly in zones experiencing urban expansion. Areas once dominated by cooler vegetation clusters are increasingly replaced by higher LST clusters, suggesting a loss of vegetative cover due to development. Despite the shrinking footprint, remaining vegetated zones (clusters 1 and 2) still exhibited a strong cooling effect, as indicated by blue and green clusters in the clustering map.

The bare land (ΔBL) clusters exhibited a moderate explanatory influence on LST, as indicated by intermediate q-statistic values derived from the Geo-detector analysis (Fig. 11c). In the clustering results, areas characterized by higher proportions of bare land correspond to clusters with moderately elevated LST values relative to vegetated clusters, reflecting the thermal properties of exposed soil and sparsely vegetated surfaces. These clusters, primarily in shades of brown and yellow (clusters 3 and 4), indicated that bare land consistently influences LST, albeit to a lesser degree than built-up areas. Nonetheless, minor shifts towards higher LST clusters can be observed in regions where bare land has encroached upon former vegetation zones. Water bodies (ΔWt) exhibited the least influence on LST, with clusters (cluster 3 and 4) primarily in cooler shades of blue and green (Fig. 11d). These clusters are concentrated in coastal and riverine areas, reflecting the water's localized cooling effect.

4 Discussion

This study advances understanding of urban ecological change in the Accra Metropolitan Area (AMA) by moving beyond descriptive assessments of land cover dynamics to an integrated, mechanism-oriented analysis of vegetation loss and surface warming. Unlike many previous studies that rely solely on historical remote sensing observations or simple correlation analyses, this research combines machine learning classification, predictive land-use modelling, and spatial heterogeneity analysis within a single analytical framework. By linking historical land cover transitions to future scenarios and explicitly quantifying their influence on land surface temperature (LST), the study provides a more comprehensive and policy-relevant interpretation of urban expansion processes. A key innovation of this work lies in its methodological integration. The combined use of

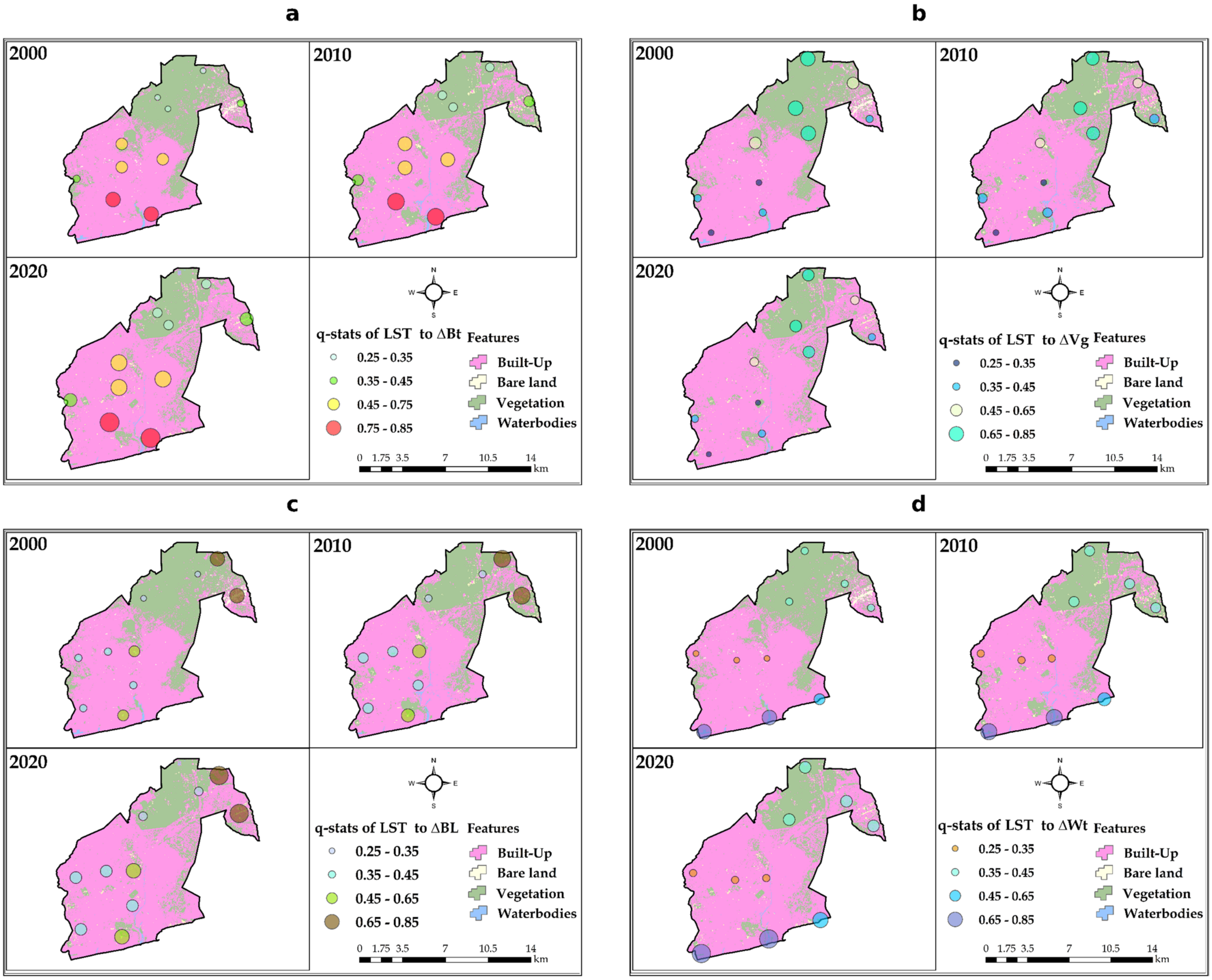

Fig. 10 q-stat results of LST spatial variations to changes in Built-Up (ΔBt), Vegetation (ΔVg), Bare land (ΔBL) and Water (ΔWt) across the two decades

random forest classification for historical LULC mapping, the MOLUSCE framework for long-term projections, and Geo-detector and K-means clustering for spatial analysis allows the identification of not only where land cover changes occur, but also how and why they influence thermal dynamics. This integrative approach moves beyond conventional correlation-based studies by explicitly revealing the mechanisms through which built-up expansion alters vegetation health and surface energy balance. Importantly, the framework is transferable and can be applied to other rapidly urbanizing cities across sub-Saharan Africa and comparable regions.

4.1 Main drivers of urban vegetation loss

The sustained conversion of vegetated surfaces into impervious built-up areas reflects intensified urban densification and spatial expansion within AMA. This restructuring of land cover reduces evapotranspirative cooling capacity and enhances heat retention, reinforcing the observed spatial patterns of elevated LST in highly urbanized zones. This trajectory reflects the combined pressures of population growth, infrastructure development, and rising demand for housing and social amenities, a pattern of rapid urbanization and its impact on green spaces that is consistently observed across the African continent and in emerging economies (Kowe and Shoko 2025). As Accra's role as Ghana's political and economic hub has intensified, green spaces have been progressively cleared to make way for residential neighborhoods, transport networks, and commercial complexes. The trend aligns with earlier findings in Ghana (Ackom et al. 2020; Biney and Boakye 2021) and parallels experiences in cities such as Yerevan, Armenia (Tepanosyan et al. 2021). However, the present study adds a new dimension by

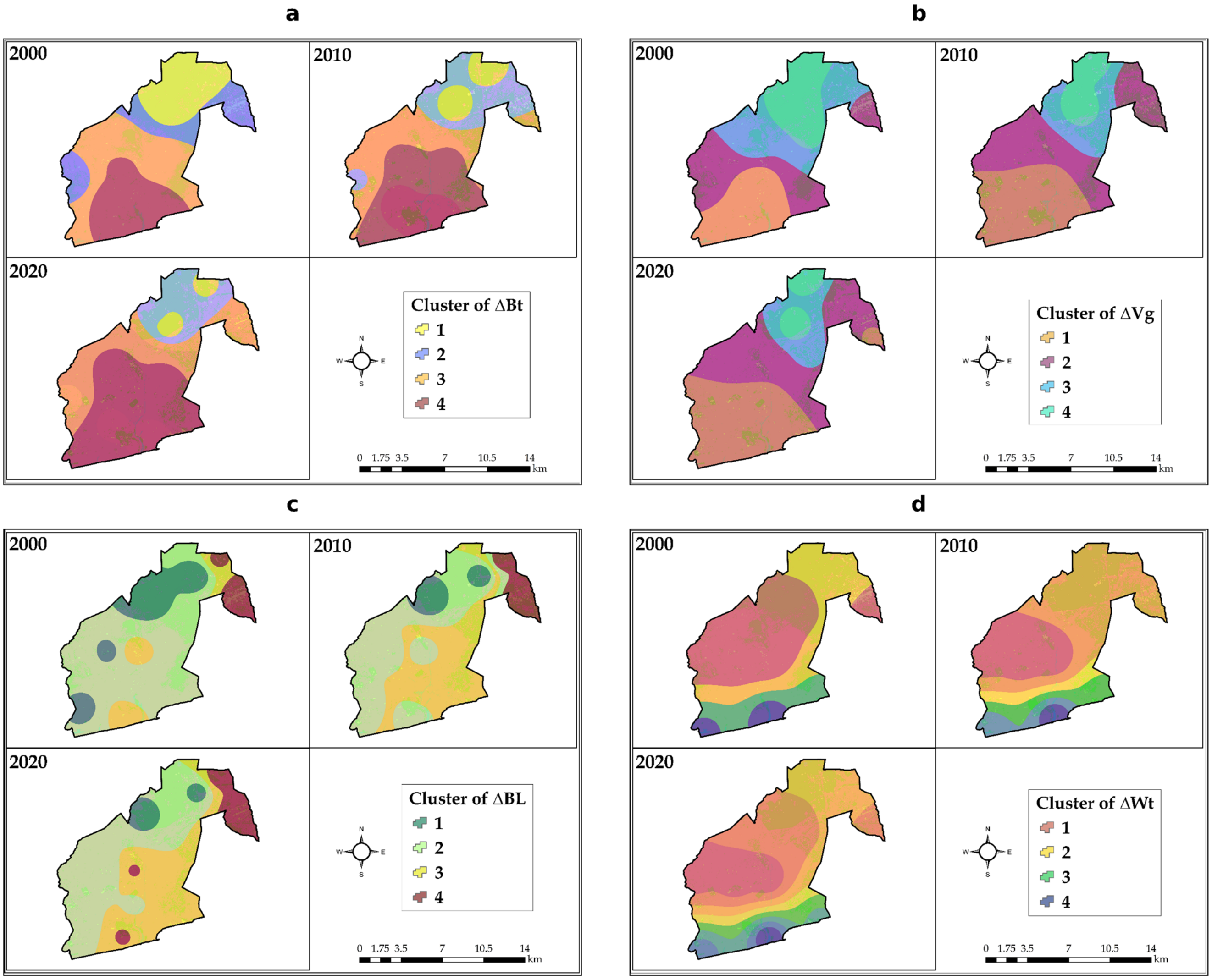

Fig. 11 K-means clustering results of LST spatial variations to changes in Built-Up (ΔBt), Vegetation (ΔVg), Bare land (ΔBl) and Water (ΔWt) across the two decades

explicitly quantifying how the conversion of vegetation to built-up surfaces explains spatial variation in LST. The Geo-detector results show that built-up areas exhibit the highest explanatory power ($q=0.75\sim0.85$), followed by vegetation cover ($q=0.65\sim0.85$), while elevation and proximity to water bodies contribute comparatively lower explanatory influence. These results indicate that urban expansion accounts for the largest share of spatial LST heterogeneity within the Accra Metropolitan Area (Fig. 11). Similar spatial analytical approaches have quantified comparable urban thermal dynamics in rapidly expanding Chinese megacities (Estoque et al. 2017; Wang et al. 2022), reinforcing the broader applicability of this framework.

Mechanistically, the drivers of vegetation loss can be explained through land–atmosphere energy interactions. Vegetation moderates local climate by shading surfaces, intercepting solar radiation, and dissipating heat via evapotranspiration. When vegetation is replaced by impervious materials such as concrete and asphalt, latent heat flux is reduced while sensible heat storage increases, a shift extensively documented in studies of urban energy balances (Sun et al. 2023; Wu et al. 2021; Yeboah et al. 2026). This energy balance shift explains the observed rise in LST in areas experiencing vegetation loss, a trend further exacerbated by broader regional climate warming as observed in Ghana (Oduro et al. 2022, 2025; Kowe et al. 2024). Moreover, higher temperatures feed back into vegetation health, causing stress, reducing photosynthetic efficiency, and further weakening vegetation's cooling capacity. This creates a reinforcing cycle: the more vegetation is lost, the more intense the heat becomes, which in turn accelerates vegetation decline (Oduro et al. 2025; Mohammad and Goswami 2021). Such feedback loops are rarely documented in AMA studies, and this research demonstrates them explicitly by integrating NDVI, NDBI, and LST into one analytical framework.

4.2 LULC prediction and its impact on the environment

Projections show that by 2050, built-up areas in AMA may account for as much as 94% of land cover, with vegetation shrinking to just 10%. This is an accelerating trend because it implies a near-complete dominance of impervious surfaces in the city's land cover, a level of urban saturation with severe ecological consequences projected for other rapidly growing cities (Anupriya et al. 2025; Yeboah et al. 2025). Unlike earlier studies that forecast changes only up to 2030, the present work extends projections two additional decades, making it, to our knowledge, one of the few studies projecting LULC dynamics for the entire Accra Metropolitan Area to 2050, extending beyond prior projections that primarily focused on 2030 or sub-basin scales. The novelty lies not only in the timeframe but also in the incorporation of multiple predictor variables, including digital elevation, transportation networks, and socio-economic factors, into the MOLUSCE model, thereby strengthening the reliability of the forecasts.

The environmental implications are severe. As vegetative cover approaches significant ecological stress, Accra will lose much of its natural cooling capacity, leading to stronger and more persistent UHI effects, with projected impacts on local climate extremes (Birungi et al. 2025; Oduro et al. 2025). The lack of vegetation will also reduce carbon sequestration, weaken soil stability, and increase vulnerability to flooding, particularly in low-lying zones already prone to waterlogging, a critical concern also identified in the Lake Victoria Basin (Birungi et al. 2025). In mechanistic terms, the disappearance of vegetation translates into a systemic alteration of the surface energy balance, where virtually all incoming solar radiation is partitioned into sensible heat, raising surface and air temperatures across the city (Yeboah et al. 2026). Once the built-up footprint reaches this projected magnitude, opportunities for large-scale ecological restoration will be extremely limited, making proactive interventions such as the strategic integration of accessible green parks (Li et al. 2022) and optimized building morphology (Sun et al. 2023) urgently necessary.

4.3 LULC changes and its impacts on NDVI, NDBI, and LST

The relationships among NDVI, NDBI, and LST in AMA provide important mechanistic evidence of how urbanization reshapes thermal and ecological systems. The strong negative correlation between NDVI and LST indicates that as vegetation cover declines, the surface temperature rises due to reduced evapotranspiration and shading, a quantitative relationship consistently demonstrated in other urban studies (Yeboah et al. 2025; Wu et al. 2021). Although cropland may exhibit seasonal differences in land surface temperature relative to continuously vegetated areas, agricultural land within the AMA is spatially limited and therefore unlikely to significantly alter the overall vegetation–LST relationship observed in this study. Conversely, the strong positive correlation between NDBI and LST shows that built-up areas amplify heating because impervious surfaces store solar energy during the day and release it slowly at night, sustaining higher temperatures, a phenomenon acutely observed in cities with dense construction (Sun et al. 2023; Kowe et al. 2022). Although built-up areas expanded over the study period, NDBI values do not increase strictly linearly across all years. In some locations, relatively higher NDBI values observed in 2010 may reflect transitional urban surfaces such as construction zones, exposed soils, and newly cleared land, which can produce strong NDBI signals. By 2020, some of these areas had transitioned into more stable built-up surfaces or mixed land cover conditions, resulting in slightly lower NDBI values despite continued urban expansion. This pattern highlights the dynamic nature of urban development, where spectral indices capture both permanent impervious surfaces and temporary land-cover transitions during different stages of urban growth. Although urban expansion generally contributes to increasing land surface temperatures, the temporal pattern of LST does not follow a strictly linear trend across the three observation years. In some areas, relatively higher LST values observed in 2010 compared to 2020 may reflect short-term variations in surface moisture conditions, seasonal climatic differences during satellite acquisition, or the presence of transitional urban surfaces such as exposed soil and construction sites that tend to heat rapidly. Such variability highlights the complex interactions between land cover dynamics and urban thermal processes. While previous studies have described correlations between land cover and LST, the present research advances the analysis by quantifying spatial stratified heterogeneity using the Geo-detector approach. Built-up areas exhibit the highest explanatory power ($q = 0.75 \sim 0.85$), followed by vegetation and other environmental variables, indicating their dominant contribution to LST spatial variation in the AMA.

The K-means clustering results provide additional mechanistic interpretation by identifying thermal hotspots concentrated in central and southern Accra. Clusters characterized by higher NDVI values and lower LST represent vegetated and relatively cooler zones, while clusters with higher NDBI and elevated LST correspond to built-up and thermally intensive areas. The vegetated and cooler zones correspond to Cluster 4 (light blue), which shows a declining spatial extent over time, reflecting vegetation loss due to urban expansion. These clusters align with zones of intensive urban development and highlight how spatial heterogeneity in land cover directly shapes urban heat dynamics. Vegetated clusters, although shrinking in extent, still serve as localized cooling areas, demonstrating the critical ecological services provided by the remaining green spaces and emphasizing the necessity of preserving and enhancing their accessibility (Li et al. 2022). Bare land clusters contribute moderately to LST increases because exposed soils heat quickly but lack the thermal inertia of built-up surfaces. Water bodies, although effective at local cooling, are too limited in area to significantly influence the city-wide thermal regime, a common limitation in many inland cities (Yeboah et al. 2025). Taking together, these findings demonstrate that the conversion of vegetation to impervious cover fundamentally alters the surface energy budget of AMA, explaining the intensification of heat islands over time, a process increasingly understood through advanced temperature monitoring (Oduro et al. 2025).

4.4 Policy recommendations

The mechanistic insights gained from this study emphasize the urgency of integrating ecological considerations into urban planning. With vegetation cover projected to decline to 10% by 2050, policy interventions must prioritize urban green infrastructure (UGI). Previous studies have demonstrated that urban vegetation and green infrastructure can significantly reduce land surface temperatures through shading and evapotranspiration processes, thereby mitigating urban heat island effects (Gill et al. 2007; Yeboah et al. 2026; Li et al. 2022; Batame et al. 2023). This includes not only traditional green spaces such as parks and community forests but also innovative solutions such as green roofs, vertical gardens, and permeable pavements that restore evapotranspiration capacity within built-up zones. Institutionalizing these measures through municipal bylaws and development codes would ensure that ecological sustainability becomes a mandatory component of urban growth.

Additionally, the application of indices such as NDVI and NDBI, combined with real-time monitoring of LST, should be institutionalized as decision-support tools for city authorities. Embedding these tools into spatial planning systems would allow for continuous tracking of vegetation decline and heat stress, enabling adaptive responses before ecological thresholds are crossed. The study's results also point to the importance of community-based interventions: public education campaigns, incentives for tree planting, and participatory neighborhood greening initiatives could help restore ecological balance while fostering civic responsibility. At the regional level, collaborations under frameworks such as the African Union's Agenda 2063 and ECOWAS Environmental Policy could provide the technical expertise and financing needed to scale up these interventions.

These findings have direct implications for the Sustainable Development Goals (SDGs), particularly SDG 11 (Sustainable Cities and Communities), SDG 13 (Climate Action), and SDG 15 (Life on Land). The observed expansion of built-up areas and the associated decline in vegetation highlight the need for urban planning strategies that integrate green infrastructure and ecosystem-based adaptation to mitigate surface warming. Protecting and restoring urban vegetation can enhance ecological resilience, moderate land surface temperatures, and reduce urban heat accumulation, thereby supporting more sustainable urban development in rapidly expanding cities such as Accra. In this context, the spatial evidence generated by this study provides a scientific basis for aligning urban land-use planning with broader sustainability and climate resilience objectives.

4.5 Limitations and future directions

Despite the advances presented in this study, certain limitations must be acknowledged. The reliance on Landsat data, while useful for long-term trend analysis, may not fully capture micro-scale dynamics in fragmented urban environments. Socioeconomic drivers of land-use change, such as informal housing growth, land tenure arrangements, and income disparities, were not explicitly modelled, even though they strongly shape urban expansion. Furthermore, the temporal resolution of the data (2000, 2010, 2020) may obscure seasonal or intra-annual dynamics of vegetation and temperature change.

Future research should build on these limitations by integrating higher-resolution imagery from Sentinel-2 or UAV platforms and coupling them with socioeconomic datasets to capture both the physical and human dimensions of urban change. Machine learning models that incorporate demographic and climatic predictors can improve the accuracy of long-term projections. Comparative studies across Ghana's other major cities, such as Kumasi, Sekondi-Takoradi, and Tamale, would also generate a broader national perspective on urban ecological transitions. Such multi-scalar approaches would provide policymakers with the evidence base needed to design urban planning strategies that balance growth with ecological resilience.

Table 6 Data sources and characteristics

Dataset	Source	Resolution	Year	Purpose
Landsat 5/7/8	USGS Earth Explorer	30 m	2000, 2010, 2020	LULC classification
DEM	SRTM	30 m	—	Topography
Roads	OpenStreetMap	Vector	—	Accessibility
Population data	GSS	Vector	2010	Urban pressure

5 Conclusions

The spatiotemporal dynamics of urban expansion and its impacts on vegetation health and LST in AMA were analyzed for the period 2000–2020, with projections extending to 2050. Integrating remote sensing, random forest classification, and MOLUSCE modelling revealed substantial land-cover restructuring, marked by a significant decline in vegetation cover from 35.7% to 22.7% and the rapid expansion of built-up areas from 62.5% to 75.6%. Projections under a business-as-usual scenario indicate this trend will intensify, with vegetation cover potentially falling to only 10.2% by 2050. The conversion of vegetated land to impervious surfaces was directly linked to increased LST, a relationship quantitatively supported by strong correlations between NDVI and LST ($r=-0.9$) and between NDBI and LST ($r=0.8$). Advanced spatial analysis further identified built-up expansion as the dominant driver of surface warming, with intensifying urban heat island effects concentrated notably in Accra's central and southern districts. Together, these results provide empirical evidence that urban growth in the AMA is systematically degrading the local ecological base and amplifying thermal stress, stressing the need for spatial planning and climate adaptation strategies informed by such evidence.

Appendix

Acknowledgements The authors would like to thank the handling editor and anonymous reviewers for their insightful comments on the manuscript.

Author contributions Conceptualization/Introduction- Michael Batame and Selasie Klutsey; Methodology- Michael Batame, Emmanuel Yeboah, and Elisha Njomaba; Software- Michael Batame and Emmanuel Yeboah; Formal Analysis- Michael Batame; LULCC Prediction- Emmanuel Yeboah; Data curation- Michael Batame and Paul Kyeku; Manuscript Draft - Michael Batame, Emmanuel Yeboah, Augustine Ohene Nyarko; Discussion- Michael Batame, Emmanuel Yeboah and Elisha Njomaba; Review and Editing— Emmanuel Yeboah, Isaac Sarfo, Oznur Isinkaralar, Muhammad Waseem, Henry Adjanor Tetteh, Ali Hasan Jaffry, Kaan Isinkaralar, Ishmeal Quist, Vincent Awuku, Kaleem Ullah and Augustine Ohene Nyarko. All authors have read and agreed to the published version of the manuscript.

Funding This research received no specific grant from any funding agency in the public, commercial, or not-for-profit sectors.

Data availability Data will be made available on request.

Code availability Code will be made available on request.

Declarations

Competing interests The authors declare no competing interests.

References

Abass K, Adanu SK, Agyemang S (2018) Peri-urbanisation and loss of arable land in Kumasi Metropolis in three decades: Evidence from remote sensing image analysis. Land use policy 72:470–479. https://doi.org/10.1016/j.landusepol.2018.01.013

Acheampong M, Yu Q, Enomah LD, Anchang J, Eduful M (2018) Land use/cover change in Ghana's oil city: Assessing the impact of neoliberal economic policies and implications for sustainable development goal number one–A remote sensing and GIS approach. Land use policy 73:373–384. https://doi.org/10.1016/j.landusepol.2018.02.019

Acheampong RA, Asabere SB, & Asuah AY (2022) Urban form and access to public transport in Accra, Ghana. In Transport andmobility futures in Urban Africa (pp. 17-31). Cham: Springer International Publishing

Ackom EK, Adjei KA, Odai SN (2020) Monitoring land-use and land-cover changes due to extensive urbanization in the Odaw River Basin of Accra, Ghana, 1991–2030. Model earth Syst Environ 6(2):1131–1143. https://doi.org/10.1007/s40808-020-00746-5

Ahmadzai MR, Zaki PH, Ismail MH, Bawon P, Karam DS (2022) The societal and economic impact of reforestation strategies and policies in Southeast Asia—A review. Forests 14(1):1. https://doi.org/10.3390/f14010001

Alademomi AS, Okolie CJ, Daramola OE, Akinnusi SA, Adediran E, Olanrewaju HO, ... & Odumosu, J (2022) The interrelationshipbetween LST, NDVI, NDBI, and land cover change in a section of Lagos metropolis, Nigeria. Applied Geomatics, 14(2), 299-314

Amekudzi E, Amponsah E, Poku-Boansi M, Anin-Yeboah OYA, & Asibey MO (2024) Decarbonizing Ghanaian cities through the lensof sustainable transportation planning: Policy and institutional response. African Transport Studies, 2, 100013

Ansah SO, Ahiataku MA, Yorke CK, Otu-Larbi F, Yahaya B, Lamptey PNL, Tanu M (2020) Meteorological analysis of floods in Ghana. Adv Meteorol 2020(1):4230627. https://doi.org/10.1155/2020/4230627

Anselmetto N, Weisberg PJ, Garbarino M (2024) Global change in the European Alps: A century of post-abandonment natural reforestation at the landscape scale. Landsc Urban Plann 243:104973. https://doi.org/10.1016/j.landurbplan.2023.104973

Anupriya RS, Rubeena TA, Geology (2025) Ecol Landscapes, 9(1), 262–278. https://doi.org/10.1080/24749508.2023.2182088

Assede ES, Orou H, Biaou SS, Geldenhuys CJ, Ahononga FC, Chirwa PW (2023) Understanding drivers of land use and land cover change in Africa: A review. Curr Landsc Ecol Rep 8(2):62–72. https://doi.org/10.1007/s40823-023-00087-w

Attua EM, Fisher JB (2011) Historical and future land-cover change in a municipality of Ghana. Earth Interact 15(9):1–26. https://doi.org/10.1175/2010EI304.1

Avdan U, Jovanovska G (2016) Algorithm for automated mapping of land surface temperature using LANDSAT 8 satellite data. J Sens 2016:1–8. https://doi.org/10.1155/2016/1480307

Awotwi A, Anornu GK., Quaye-Ballard JA, & Annor T (2018) Monitoring land use and land cover changes due to extensive goldmining, urban expansion, and agriculture in the Pra River Basin of Ghana, 1986–2025. Land degradation & development, 29(10), 3331-3343

Awuah KGB, Abdulai RT (2022) Urban land and development management in a challenged developing world: an overview of new reflections. Land 11(1):129. https://doi.org/10.3390/land11010129

Batame M, Sarfo I, Yeboah E, Njomaba E, Puplampu DA (2023) Mapping of sacred groves in Ghana: the case of Talensi district in the guinea ecological zone. SN Social Sci 3(9):145. https://doi.org/10.1007/s43545-023-00737-0

Baye F (2025) Informal land market mechanisms for accessing and securing land for housing development: the case of peri-urban areas of Woldia Township, Ethiopia. Cogent Social Sci 11(1):2482115. https://doi.org/10.1080/23311886.2025.2482115

Bhattarai K, & Conway D (2020) Urban growth. In Contemporary environmental problems in Nepal: Geographic perspectives (pp. 201-334). Cham: Springer International Publishing

Biney E, Boakye E (2021) Urban sprawl and its impact on land use land cover dynamics of Sekondi-Takoradi metropolitan assembly. Ghana Environ Challenges 4:100168. https://doi.org/10.1016/j.envc.2021.100168

Birungi J, Yu J, Yeboah E, King'uza PH, Jonah K (2025) Impact of land-use changes on the increase in extreme precipitation events in the Lake Victoria Basin. Urban Clim 64:102615. https://doi.org/10.1016/j.uclim.2025.102615

Breiman L (2001) Random forests. Mach Learn 45(1):5–32. https://doi.org/10.1023/A:1010933404324

Chithra K, Anilkumar PP, & Naseer MA (2016) Municipal solid waste management, a major impacted sector of urban environment dueto residential land use activities-study of Kozhikode City. Procedia Environmental Sciences, 35, 110-118

Cobbinah PB, Aboagye HN (2017) A Ghanaian twist to urban sprawl. Land use policy 61:231–241. https://doi.org/10.1016/j.landusepol.2016.10.047

Cobbinah P, Brandful EG, Owusu-Amponsah L (2015) Peri-urban morphology and indigenous livelihoods in Ghana. Habitat Int 50:120–129. https://doi.org/10.1016/j.habitatint.2015.08.002

Coll C, Galve JM, Sanchez JM, Caselles V (2010) Validation of Landsat-7/ETM+ Thermal-Band Calibration and Atmospheric Correction With Ground-Based Measurements. IEEE Trans Geosci Remote Sens 48:547–555. https://doi.org/10.1109/tgrs.2009.2024934

Enescu CM, Mihalache M, Ilie L, Dinca L, Chira D, Vasić A, Murariu G (2025) Advancing the Sustainability of Poplar-Based Agroforestry: Key Knowledge Gaps and Future Pathways. Sustainability 18(1):341. https://doi.org/10.3390/su18010341

Estoque RC, Murayama Y, Myint SW (2017) Effects of landscape composition and pattern on land surface temperature: An urban heat island study in the megacities of Southeast Asia. Sci Total Environ 577:349–359. https://doi.org/10.1016/j.scitotenv.2016.10.195

Faisal BR, Rahman H, Sharifee NH, Sultana N, Islam MI, Habib SA, Ahammad T (2020) Integrated application of remote sensing and GIS in crop information system—a case study on aman rice production forecasting using MODIS-NDVI in Bangladesh. AgriEngineering 2(2):264–279. https://doi.org/10.3390/agriengineering2020017

Frimpong A, Kwabena Forkuo E, & Matthew Osei Jnr E (2024b). The effect of land use land cover types on MODIS land surface temperature in Ghana. Cogent Engineering 11(1), 2411865

Frimpong LK, Mensah SL, & Ablo AD (2024a) Households' access and expenditure on water services: Examining intra-urbandifferences in the Accra metropolis, Ghana. Urban Governance 4(3), 222-231

Ghana. Statistical Service (2014) 2010 Population & housing census report: Disability in Ghana. Ghana Statistical Service

Ghulam A, Hall M (2010) Calculating surface temperature using Landsat thermal imagery. Online: https://serc.carleton.edu/files/NAGTWorkshops/gis/activities2/student_handout_calculating_te.pdf Accessed 25 Mar 2016

Gill SE, Handley JF, Ennos AR, Pauleit S (2007) Adapting cities for climate change: the role of the green infrastructure. Built Environ 33(1):115–133. https://doi.org/10.2148/benv.33.1.115

Grant R, Nijman J (2004) The re-scaling of uneven development in Ghana and India. Tijdschrift voor economische en sociale geografie. 95(5):467–481. https://doi.org/10.1111/j.0040-747X.2004.00333.x

Grant R, Yankson P (2003) Accra Cities 20(1):65–74. https://doi.org/10.1016/S0264-2751(02)00090-2

Hu Y, Raza A, Syed NR, Acharki S, Ray RL, Hussain S, Dehghanisanij H, Zubair M, Elbeltagi A (2023) Land use/land cover change detection and NDVI estimation in Pakistan's Southern Punjab Province. Sustainability 15(4):3572. https://doi.org/10.3390/su15043572

Isinkaralar O, Isinkaralar K, Yilmaz D (2023) Climate-related spatial reduction risk of agricultural lands on the Mediterranean coast in Türkiye and scenario-based modelling of urban growth. Environ Dev Sustain 25(11):13199–13217. https://doi.org/10.1007/s10668-023-03774-0

Kamaraj M, Rangarajan S (2022) Predicting the future land use and land cover changes for Bhavani basin, Tamil Nadu, India, using QGIS MOLUSCE plugin. Environ Sci Pollut Res 29(57):86337–86348. https://doi.org/10.1007/s11356-021-17904-6

Kowe P, Shoko C (2025) A spatial autocorrelation approach in examining the impacts of spatial-temporal dynamics of seasonal land surface temperature and land cover changes on the urban climate of the metropolitan city of Bulawayo. J Spat Sci 70(4):621–642. https://doi.org/10.1080/14498596.2025.2570646

Kowe P, Mutanga O, Odindi J, Dube T (2021) Effect of landscape pattern and spatial configuration of vegetation patches on urban warming and cooling in Harare metropolitan city. Zimbabwe GIScience Remote Sens 58(2):261–280. https://doi.org/10.1080/15481603.2021.1877008

Kowe P, Dube T, Mushore TD, Ncube A, Nyenda T, Mutowo G, Kizilirmak G (2022) Impacts of the spatial configuration of built-up areas and urban vegetation on land surface temperature using spectral and local spatial autocorrelation indices. Remote Sens Lett 13(12):1222–1235. https://doi.org/10.1080/2150704X.2022.2142073

Kowe P, Mutanga O, Odindi J, Dube T (2024) Impacts of eco-environmental quality, spatial configuration, and landscape connectivity of urban vegetation patterns on seasonal land surface temperature in Harare metropolitan city. Zimbabwe Afr Geographical Rev 43(1):125–143. https://doi.org/10.1080/19376812.2022.2117215

Li X, Stringer LC, Dallimer M (2022) The impacts of urbanisation and climate change on the urban thermal environment in Africa. Climate 10(11):164. https://doi.org/10.3390/cli10110164

Liu T, Yu L, Yan Z, Li X, Bu K, Yang J (2025) Enhanced climate mitigation feedbacks by wetland vegetation in semi-arid compared to humid regions. Geophys Res Lett 52(9):e2025GL115242 https://doi.org/10.1029/2025GL115242

McManamay R A, Raad A, Vernon CR., Thurber T, Gao J, Powers S, & O'Neill B (2024) Divergent urban land trajectories underalternative population projections within the Shared Socioeconomic Pathways. Environmental Research Letters 19(4), 044025

Mir YH, Mir S, Ganie MA, Bhat JA, Shah AM, Mushtaq M, Irshad I (2025) Overview of land use and land cover change and its impacts on natural resources. Ecologically mediated development: Promoting biodiversity conservation and food security. Springer, Singapore, pp 101–130. https://doi.org/10.1007/978-981-96-2413-3_5Nature Singapore

Mohammad P, Goswami A (2021) Quantifying diurnal and seasonal variation of surface urban heat island intensity and its associated determinants across different climatic zones over Indian cities. GIScience Remote Sens 58(7):955–981. https://doi.org/10.1080/15481603.2021.1940739

Muhammad R, Zhang W, Abbas Z, Guo F, Gwiazdzinski L (2022) Spatiotemporal change analysis and prediction of future land use and land cover changes using QGIS MOLUSCE plugin and remote sensing big data: a case study of Linyi China. Land 11(3):419. https://doi.org/10.3390/land11030419

Myers G (2021) Urbanisation in the global south. Urban ecology in the global south. Springer International Publishing, Cham, pp 27–49. https://doi.org/10.1007/978-3-030-67650-6_2

Oduro C, Shuoben B, Ayugi B, Beibei L, Babaousmail H, Sarfo I, Ngoma H (2022) Observed and Coupled Model Intercomparison Project 6 multimodel simulated changes in near-surface temperature properties over Ghana during the 20th century. Int J Climatol 42(7):3681–3701. https://doi.org/10.1002/joc.7439

Oduro C, Lim Kam Sian KTC, Hagan DFT, Babaousmail H, Ayugi BO, Wu Y, Wu N (2025) The influence of land surface temperature on Ghana's climate variability and implications for sustainable development. Sci Rep 15(1):2595. https://doi.org/10.1038/s41598-025-86585-9

Owusu AB, Mensah CA, Fynn IEM, Kwang C, Arthur IK, Adu-Boahen K (2023) Indicator-based assessment of the liveability of communities in the Accra Metropolitan Area, Ghana: A transdisciplinary approach. Social Sci Humanit Open 8(1):100702. https://doi.org/10.1016/j.ssaho.2023.100702

Sarfo I, Shuoben B, Beibei L, Amankwah SOY, Yeboah E, Koku JE, Nunoo EK, Kwang C (2022) Spatiotemporal development of land use systems, influences and climate variability in Southwestern Ghana (1970–2020). Environ Dev Sustain, 1–33. https://doi.org/10.1007/s10668-021-01848-5

Sarfo I, Bi S, Kwang C, Yeboah E, Addai FK, Nkunzimana A, Ofori MA, Batame M, Appea EA, Asiedu A (2023a) Class dynamics and relationship between land-use systems and surface temperature in south-eastern Ghana. Environ Earth Sci 82(4):104. https://doi.org/10.1007/s12665-023-10755-z

Sarfo I, Bi S, Xu X, Yeboah E, Kwang C, Batame M, Addai FK, Adamu UW, Appea EA, Djan MA (2023b) Planning for cooler cities in Ghana: Contribution of green infrastructure to urban heat mitigation in Kumasi Metropolis. Land use policy 133:106842. https://doi.org/10.1016/j.landusepol.2023.106842

Sarfo I, Qiao J, Yeboah E, Puplampu DA, Kwang C, Fynn IEM, Batame M, Appea EA, Hagan DFT, Ayelazuno RA (2024) Meta-analysis of land use systems development in Africa: Trajectories, implications, adaptive capacity, and future dynamics. Land use policy 144:107261. https://doi.org/10.1016/j.landusepol.2024.107261

Seto KC, Parnell S, Elmqvist T (2013) A global outlook on urbanization. Urbanization, biodiversity and ecosystem services: challenges and opportunities: a global assessment. Springer Netherlands, Dordrecht, pp 1–12. https://doi.org/10.1007/978-94-007-7088-1_1

Songsore J (2020) The urban transition in Ghana: Urbanization, national development and poverty reduction. Ghana Social ScienceJournal 17(2), 57-57.

Sun J, Yang K, Yu Y, Lu H, Lin Y (2023) Land–atmosphere interactions partially offset the accelerated Tibetan Plateau water cycle through dynamical processes. J Clim 36(11):3867–3880. https://doi.org/10.1175/JCLI-D-22-0686.1

Tan Z, Lau KKL, Ng E (2016) Urban tree design approaches for mitigating daytime urban heat island effects in a high-density urban environment. Energy Build 114:265–274. https://doi.org/10.1016/j.enbuild.2015.06.031

Tepanosyan G, Muradyan V, Hovsepyan A, Pinigin G, Medvedev A, Asmaryan S (2021) Studying spatial-temporal changes and relationship of land cover and surface Urban Heat Island derived through remote sensing in Yerevan. Armen Building Environ 187:107390. https://doi.org/10.1016/j.buildenv.2020.107390

Wang C, Ren Z, Dong Y, Zhang P, Guo Y, Wang W, Bao G (2022) Efficient cooling of cities at global scale using urban green space to mitigate urban heat island effects in different climatic regions. Urban Urban Green 74:127635. https://doi.org/10.1016/j.ufug.2022.127635

Wu H, Wang T, Wang QG, Cao Y, Qu Y, Nie D (2021) Radiative effects and chemical compositions of fine particles modulating urban heat island in Nanjing, China. Atmos Environ 247:118201. https://doi.org/10.1016/j.atmosenv.2021.118201

Yeboah E, Sarfo I, Kwang C, Alimo PK, Djan MA, Afenya MS, Amankwah SOY (2025) Influence of land use patterns on urban heat island dynamics in an emerging megacity: a case study of Zhengzhou, Henan, China. J Chin Archit Urbanism 8412. https://doi.org/10.36922/jcau.8412

Yeboah E, Hagan DFT, Wang G, Cabral P, Sarfo I, Bediako-Kyeremeh B, Hu Y (2026) Understanding the causal influence of energy balance components on urban heat islands in a mid-latitude city-Chongqing. China Urban Clim 65:102735. https://doi.org/10.1016/j.uclim.2025.102735

Yiran G, Kusimi J, Kufogbe S (2012) A synthesis of remote sensing and local knowledge approaches in land degradation assessment in the Bawku East District, Ghana. Int J Appl Earth Obs Geoinf 14(1):204–213. https://doi.org/10.1016/j.jag.2011.09.016

Yiran GAB, Ablo AD, Asem FE (2020) Urbanisation and domestic energy trends: Analysis of household energy consumption patterns in relation to land-use change in peri-urban Accra, Ghana. Land Use Policy 99:105047. https://doi.org/10.1016/j.landusepol.2020.105047

Zhang X, Wu S, Yan X, Chen Z (2017) A global classification of vegetation based on NDVI, rainfall and temperature. Int J Climatol 37(5):2318–2324. https://doi.org/10.1002/joc.4847

Zhang M, Kafy A-A, Xiao P, Han S, Zou S, Saha M, Zhang C, Tan S (2023) Impact of urban expansion on land surface temperature and carbon emissions using machine learning algorithms in Wuhan, China. Urban Clim 47:101347. https://doi.org/10.1016/j.uclim.2022.101347

Authors and Affiliations

Michael Batame[1] · Emmanuel Yeboah[2] · Elisha Njomaba[3] · Isaac Sarfo[4,13] · Selasi Klutsey[5] · Oznur Isinkaralar[6] · Muhammad Waseem[7,14] · Ali Hasan Jaffry[2] · Kaan Isinkaralar[8] · Henry Adjanor Tetteh[9] · Paul Kyeku[10] · Ishmeal Quist[11] · Vincent Awuku[12] · Kaleem Ullah[2] · Augustine O. K. N. Mensah[11]

✉ Emmanuel Yeboah
emmanuelyeboah@nuist.edu.cn

✉ Augustine O. K. N. Mensah
aoknmensah@nuist.edu.cn

Michael Batame
michaelbatame8@gmail.com

Elisha Njomaba
njomaba@fld.czu.cz

Isaac Sarfo
isaacsarfo@henu.edu.cn

Selasi Klutsey
selasiklutsey10@gmail.com

Oznur Isinkaralar
obulan@kastamonu.edu.tr

Muhammad Waseem
dr.waseem@uet.edu.pk

Ali Hasan Jaffry
alijafrey1122@gmail.com

Kaan Isinkaralar
kisinkaralar@kastamonu.edu.tr

Henry Adjanor Tetteh
adhinortey@gmail.com

Paul Kyeku
pkyeku8@gmail.com

Ishmeal Quist
202451290003@nuist.edu.cn

Vincent Awuku
vincentawuku@gmail.com

Kaleem Ullah
202351540001@nuist.edu.cn

1 Warnell School of Forestry and Natural Resources, University of Georgia, GA 30602, Athens, USA

2 School of Remote Sensing and Geomatic Engineering Nanjing University of Information Science and Technology, Nanjing, Jiangsu 210044 , China

3 Faculty of Forestry and Wood Sciences, Czech University of Life Sciences, Prague, Czech Republic

4 College of Geographical Science and Engineering, Henan University, Kaifeng, Henan Province 475004, China

5 School of Geography, University of Leeds, Woodhouse, UK

6 Department of Landscape Architecture, Faculty of Engineering and Architecture, Kastamonu University, Kastamonu 37150, Turkey

7 College of Hydrology and Water Resources, Hohai University, Nanjing 210098, China

8 Department of Environmental Engineering, Faculty of Engineering and Architecture, Kastamonu University, Kastamonu 37150, Turkey

9 Department of Land Administration, Faculty of Geoinformation Science and Earth Observation, ITC, University of Twente, Enschede, Netherlands

10 Department of Earth, Atmospheric, and Geographic Information Science, Western Illinois University, Macomb, IL, USA

11 School of Law and Public Administration, Research Institute for History of Science and Technology, Nanjing University of Information Science and Technology, Nanjing, Jiangsu 210044, China

12 Jiangsu Key Laboratory of Atmospheric Environment Monitoring and Pollution Control, Collaborative Innovation Center of Atmospheric Environment and Equipment Technology, School of Environment Science & Engineering, Nanjing University of Information Science & Technology, Nanjing 210044, China

13 Organization of African Academic Doctors (OAAD), Off Kamiti Road, P.O. Box 25305000100, Nairobi, Kenya

14 Centre of Excellence in Water Resources Engineering, University of Engineering and Technology, Lahore 54890, Pakistan